



New Zealand kauri trees – Identification and canopy stress analysis with optical remote sensing and LiDAR data

Research project between the University of Canterbury and the Ministry for Primary Industries / Kauri Dieback Programme

Final report v.02

updated June 2020

Jane Meiforth
UNIVERSITY OF CANTERBURY



Report version

The first version of this report from December 2018 was updated in June 2020 according to the findings published in Meiforth et al. 1999 and 2020a and 2020b:

Meiforth, J.J.; Buddenbaum, H.; Hill, J.; Shepherd, J.; Norton, D.A. Detection of New Zealand Kauri Trees with AISA Aerial Hyperspectral Data for Use in Multispectral Monitoring. *Remote Sensing*. 2019, 11, 2865. <https://doi.org/10.3390/rs11232865> [1]

Meiforth, J.J.; Buddenbaum, H.; Hill, J.; Shepherd, J. Monitoring of Canopy Stress Symptoms in New Zealand Kauri Trees Analyzed with AISA Hyperspectral Data. *Remote Sensing*. 2020a, 12, 926. <https://doi.org/10.3390/rs12060926> [2]

Meiforth, J.J.; Buddenbaum, H.; Hill, J.; Shepherd, J.; Dymond J. 2020: Stress Detection in New Zealand Kauri Canopies with WorldView-2 Satellite and LiDAR Data. *Remote Sensing*. 2020b, 12, 1906. <https://doi.org/10.3390/rs12121906> [3]

Contact

Researcher: Jane J. Meiforth, jane.meiforth@pg.canterbury.ac.nz

Doctoral candidate, GIS Analyst (PgD) and Grad. Eng. for Nature Management & Landscape Planning

Ministry for Primary Industries: Travis Ashcroft, Senior Adviser, Long-term Programmes,
Travis.Ashcroft@mpi.govt.nz

Supporters of the project/PhD: See attachment 7.1

Funding

The Ministry of Primary Industries funded most of the remote sensing data (agreement No. 17766). The University of Canterbury, the University of Trier and FrontierSI (former CRC SI) Australia provided scholarships for living costs, fieldwork, equipment and additional LiDAR data. Digital Globe and Blackbridge helped with grants for satellite data. Auckland Council supported the fieldwork and supplied LiDAR data, and aerial images and Manaaki Whenua Landcare Research provided field equipment. Rapidlasso and Harris Geospatial helped with grants for software licenses. Henning Buddenbaum was supported within the framework of the EnMAP project (FKZ 50 EE 1530) by the German Aerospace Center (DLR) and the Federal Ministry of Economic Affairs and Energy. The publications were funded by Manaaki Whenua Landcare Research and the Open Access Fund of Universität Trier and the German Research Foundation (DFG) within the Open Access Publishing funding programme.

Image on the front page

View from the Fenceline track in the Waitakere Ranges, summer 2016

Table of Contents

1	SUMMARY	4
2	INTRODUCTION	6
2.1	Background of the project	6
2.2	Objective	6
2.3	Framework	6
2.4	Area	7
2.5	Data and software	7
3	RESULTS	13
3.1	Spectral characteristics of kauri and separability from other species	13
3.2	Kauri identification	15
3.3	Detect symptoms of stress in the canopy	22
3.4	Automatic stand and crown segmentation	32
3.5	Main challenges and lessons learned	36
4	CONCLUSIONS AND OUTLOOK	37
5	ABBREVIATIONS	39
6	REFERENCES	40
7	APPENDIX	43
7.1	Support for the project	43
7.2	LiDAR data	44
7.3	Assessment scheme for stress symptoms in kauri crowns	45
7.4	Kauri detection – images and maps	46

Tableaus with illustrations

Tableau 1: Study area, remote sensing data	8
Tableau 2: Field reference data	10
Tableau 3: Phenology of kauri and neighbouring tree species	12
Tableau 4: Kauri spectral characteristics and separability from other canopy species	14
Tableau 5: Hyperspectral data preparation	16
Tableau 6: Kauri identification with 5 selected bands	18
Tableau 7: Kauri identification: WorldView-2 satellite data	20
Tableau 8: Kauri identification: Optical & LiDAR data (crown-based)	21
Tableau 9: Stress symptoms in the kauri spectra	23
Tableau 10: Detection of stress symptoms with selected vegetation indices	26
Tableau 11: Detection of stress symptoms with a WorldView-2 image	29
Tableau 12: Improving optical stress analysis with LiDAR data	31
Tableau 13: Stand segmentation on LiDAR data	33
Tableau 14: Crown segmentation on LiDAR data	35

Acknowledgement

My sincere thanks go to all people who enabled this project. I like to thank my supervisors Professor Joachim Hill, Professor David Norton and Dr Henning Buddenbaum, for their patient support and valuable advice. I would also like to extend my thanks to Dr James Shepherd from Landcare Research for his support during the fieldwork and the analysis. This project would not have been possible without the assistance on the ground for the work and data collection in the Waitakere Ranges. I am especially grateful to Yue Chin Chew, Dr Nick Waipara and Lee Hill from Auckland Council, who helped to establish the project and provided data and support for the fieldwork. I would also like to thank the staff of the Arataki visitor centre, Fredrik Hjelm from Biosense / The Living Tree Company and Dr Joanne Peace for their excellent help and guidance during the fieldwork. And I like to thank the Kauri Dieback Programme (Planning and Intelligence Team) for constructive feedback and support during this research. Dr Justin Morgenroth (University of Trier) and Dr Michael Watt (Scion) were involved in the first part of the project. I enjoyed our discussions and hope that we can cooperate in the future. Both the setup at two Universities, the extensive data collection and technical delays etc. posed challenges to the administration. My special thanks go to Univ.-Prof. Bruce Manley, Jeanette Allen, Vicki Wilton and Michelle van Rheede at the University of Canterbury, as well as Nichole Gellner, Dr Achim Röder and Dr Johannes Stoffels at the University of Trier for their patience and professional support to master the administrative procedures and requirements.

1 Summary

The endemic New Zealand kauri trees (*Agathis australis* (D.Don) Lindl.) are under threat by the kauri dieback disease caused by the pathogen *Phytophthora agathidicida* (PA). This project aims to develop a method based on remote sensing data to identify the location of kauri trees in forest areas and analyze the level of stress symptoms in the canopy. The Kauri Dieback Programme financed most of the research costs. The project is part of a PhD at the University of Canterbury and the University of Trier in Germany.

The analysis is based on LiDAR data, RGB aerial images, a WorldView-2 image and an AISA Fenix hyperspectral image. The data was captured for three study sites in the Waitakere Ranges west of Auckland. Reference data for over 3800 crown positions and attributes were gathered during fieldwork and from aerial images. However, the number of crowns used as a reference in the different parts of the analysis varied according to the task and dataset. In high and dense forest stands, high resolution RGB aerial images ($\leq 15\text{cm}$ pixels size) from the same season are better suited to assess stress symptoms in the canopy than a ground assessment.

Spectral characteristics

Kauri canopies with no visible symptoms show distinct spectral characteristics in the far near-infrared spectral bands. These are usually not integrated with standard multispectral sensors. The signature of small kauri crowns differs slightly from larger crowns with more open canopies. The spectral separability to 21 other canopy species respective species groups is generally good. However, outliers caused by dead branches, epiphytes, shadow effects and mixed pixels in small crowns lead to confusion. Symptomatic kauri crowns show characteristic spectral features of decline that indicate reduced leaf water, reduced chlorophyll, reduced biomass and an increase in dry matter and visible carotenoids in the leaf pigments. These features can be described with spectral indices.

Kauri identification

For the identification of a combined class of "kauri and dead/dying trees" from "other canopy vegetation", a selection of indices from five spectral bands resulted in a pixel-based accuracy of 93.8% based on a representative set of 3165 crowns. The full hyperspectral range resulted in a 96.2% pixel-based accuracy. With only standard bands in the visible to first near-infrared (VNIR1), a combination with LiDAR attributes improved the classification results significantly in a crown-based analysis. On a reduced set of 1216 crowns, the LiDAR attributes improved the accuracy for an airborne VNIR1 multispectral sensor to 91.7%, from 83.1% without LiDAR data. In combination with WorldView-2 satellite data, additional LiDAR attributes enhanced the accuracy to 91%, compared to 82.9% without LiDAR data. However, when far near-infrared bands with the most characteristic spectral features for kauri are available, additional LiDAR attributes do not substantially improve the accuracy. A test with two stripes of data from the same LiDAR sensor that was used for the Northland flights (5.8 returns/m²) gave comparable results.

Stress detection

For the detection of stress symptoms with the 1 m pixel size of the AISA image, a minimum crown size of 3 m mean diameter was defined. The analysis was based on a Random Forest regression for the description of five stress symptom levels from 1 = non-symptomatic to 5 = dead. A combination of five indices on six bands in the visible to the near-infrared region (450–970 nm) achieved a correlation of 0.93. Individual models for pre-segmented low and high forest stands improved the overall performance. A method for an automatic crown- and stand-segmentation based on LiDAR height models was developed and should be further improved for large-area application.

On the full spectral range, additional indices in the far near-infrared and short wave infrared region were selected that are sensitive to leaf water content, leaf nitrogen and cellulose / dry matter. They enhanced the correlation slightly to 0.94. However, these bands are located in spectral regions that are usually not captured by standard airborne multispectral sensors.

A crown size of 4 m mean diameter was defined as the recommended minimum size for the use of the WV2 image for stress detection, to avoid mixed pixels and to identify dying top branches in small crowns. Smaller crowns should be analyzed in homogenous stand units. A selection of eight WV2 attributes resulted in a correlation of 0.89 in a crown-based Random Forest regression. In addition to the multispectral bands, the maximum crown height value from the LiDAR data was included in the analysis to allow for a size stratification.

The resulting symptom classes need to be interpreted to relate them to the health state of the tree. The interpretation should consider the crown size, the growing conditions, proximity to infected stands and seasonal drought conditions.

Conclusions

For the kauri identification, a sensor with five selected multispectral bands in the visible to far near-infrared spectral region is recommended. The pixel resolution should ideally be $\leq 0.5\text{m}$, to cover smaller crowns. Alternatively, a standard sensor with bands in the visible to the first near-infrared spectral range should be combined with LiDAR attributes in a crown-based analysis on accurately segmented crown polygons.

For regular monitoring of stress symptoms, the spectral resolution of a WorldView-2 image is sufficient. When a WorldView-2 image is used, the reporting units for crowns smaller 4 m diameter should be aggregated in homogenous stand polygons, and the image should be taken with a high sun elevation to avoid internal shadows. More detailed correlations to certain types of stress and a crown-based analysis in small stands require a finer spectral and spatial resolution from an airborne acquisition.

2 Introduction

2.1 Background of the project

New Zealand kauri (*Agathis australis*) on the Northern Island are important natural features of New Zealand's indigenous forests, of high cultural significance for Māori and a major tourist attraction [4]. The pathogen of kauri dieback disease (*Phytophthora agathidicida* (PA)) was first confirmed in 2008 in the Waitakere Ranges [5]. But there is evidence that the pathogen has affected kauri in New Zealand already for decades [6-8]. Meanwhile, it has become a significant threat for kauri trees in New Zealand [9].

While the main distribution of kauri and PA, at broad-scales, is known, there is a need for more detailed, objective surveillance and mapping of existing kauri trees and infected sites [10,11]. Current monitoring programs are mainly based on fieldwork and photos taken from plane and helicopter [12,13].

2.2 Objective

The main objective is to develop a method based on remote sensing data to identify kauri trees and symptoms of stress in the upper canopy that can be caused by PA. The study was designed to result in recommendations to support cost-effective monitoring that can be applied to larger areas.

The process is structured in three tasks:

1. Kauri identification,
2. Detection of symptoms of stress in the upper canopy,
3. Segmentation of stands and crown polygons.

Remote sensing can describe stress symptoms in the canopy. However, it cannot prove the infection with PA. These stress symptoms can have many causes like drought, and a PA infection is just one of them. Spectral indices can characterize the type of stress like nutrient deficiency, loss of leaf water and loss of biomass. An assessment of kauri health requires an interpretation of the detected stress symptoms with local knowledge and other surveillance results.

2.3 Framework

The project is part of a PhD at the University of Canterbury in New Zealand and the University of Trier in Germany. The Kauri Dieback Program at the Ministry for Primary Industries financed most of the research costs, including most of the remote sensing data. Appendix 7.1 gives an overview of the supporters and supervisors of the project.

2.4 Area

The Waitakere Ranges, northwest of central Auckland, were chosen as the study area because they cover a wide range of kauri trees in different growth and health classes in a range of different ecotypes [14]. Existing aerial images and LiDAR data and the ongoing fieldwork of Auckland Council provided a good base to prepare the study [12,15].

Three sites in the Waitakere Ranges Heritage Area (Maungaroa 5.4 km², Kauri Grove 1.1 km² and Cascades 10.3 km²) were identified as suitable test areas for the data acquisition— see map in Tableau 1. They cover a representative selection of the major forest ecotypes with kauri in the Waitakere [14].

A rough terrain characterizes the Waitakere Ranges from sea level to a maximum altitude of 336 m in the study sites. The climate is warm-temperate with humid winds from the sea [16]. Walking tracks allowed access to the investigated forest stands.

2.5 Data and software

2.5.1 Remote sensing and other spatial data

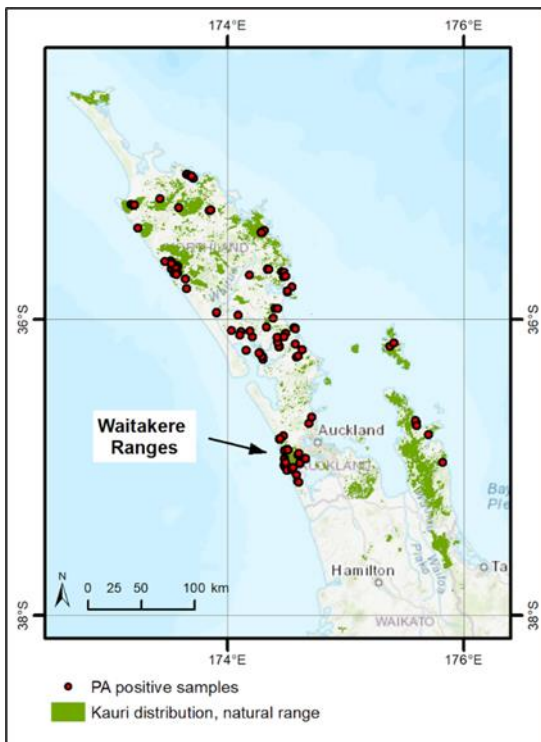
The following remote sensing data was used for the analysis:

- LiDAR data 2016: Dataset with five pulses/m² and 35 returns/m² on average, 0.17 m average point spacing, flown on the 30th of January 2016 by AAM NZ with a Q1560 LiDAR sensor (Appendix 7.2).
- LiDAR data 2018: Two LiDAR stripes with the sensor for the Northland flight, acquired by RPS Australia (Appendix 7.2).
- Aerial image 2016: RGB bands, 15 cm pixel resolution, acquired together with the LiDAR data on the 30th of January 2016, delivered in two versions: Orthorectified on the terrain and the surface model.
- Aerial image 2017: 3 band RGB, 7.5 cm resolution. Acquired between February and June 2017 by Auckland Council. Orthorectified on the terrain model.
- Hyperspectral data: AISA Fenix sensor, 448 spectral bands (352 bands usable), 1 m spatial resolution, acquired on the 15th of March 2017 by Massey University.
- Satellite image: WorldView-2 image, eight multispectral bands with a 1.8 m nadir pixel resolution, a PAN channel with a 0.45 m resolution, 15th of March 2017, cloud-free conditions.

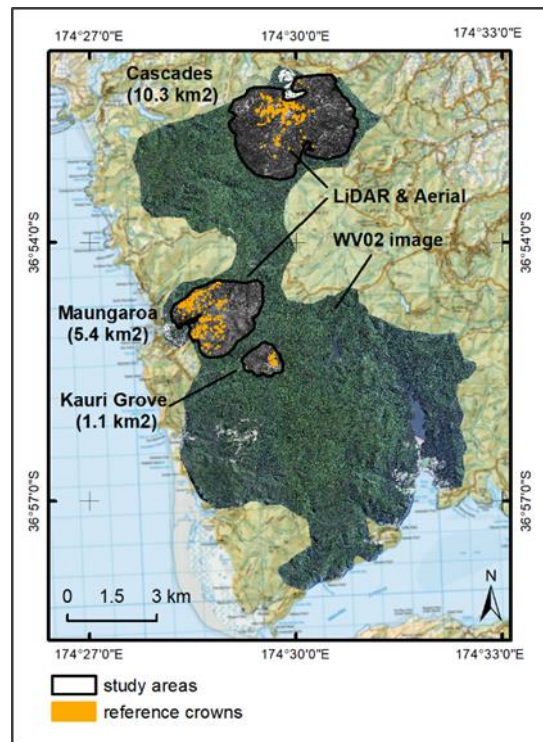
The following data sources were used as base maps and background information:

- Topographical data like streets, tracks, land cover, houses etc. from LINZ [17].
- Weather and climate data from the NZ Meteorological service [18].
- Auckland Council data from ground truthing surveys on kauri dieback in the years 2008 – 2014 [19].
- Auckland Council: Walking tracks in the Waitakere Ranges. [20]

Tableau 1: Study area, remote sensing data



Map: Location of the Waitakere Ranges on the North Island of New Zealand west of Auckland City, with the natural range of kauri distribution and PA-positive samples. [21,22].



Map: Study sites and extent of the remote sensing datasets in the Waitakere Ranges, with the reference crowns marked in orange (background map: [23]).



Cascade area:
Some small, mainly medium to large kauri stands both infected and not infected



Maungaroa area / Home Track:
Small stands, partly highly infected



Kauri Grove area
Large kauri and other large canopy species

Photos: Helicopter pictures, flown by Wild Earth Media, Auckland Council 2016 [24].

2.5.2 Field reference data

During the fieldwork in 2016 and 2017, reference crowns were mapped in circular sampling plots for denser stands and directly edited on a field tablet for easy to identify tree crowns in open stands (Tableau 2). The recorded attributes in the field include the species or species group and the position for all crowns. In circular stands and for kauri trees, additional attributes were recorded like the diameter, estimated density and coverage, optical characteristics like yellowing of leaves, the per cent of dead branches, an overall classification of the stress symptoms in the canopy (1= no symptoms to 5=dead) and anomalies like epiphytes or double stems. The circular sampling plot method required two people. In summer 2017, the symptom classes of the kauri trees were updated, and additional crowns were added in the field. The crown polygons were edited on the LiDAR height models. A 10% diameter buffer was subtracted from the outer edge of the crowns to avoid edge effects in the analysis. The high-resolution aerial images that became available at the end of 2016 and 2017 allowed the further editing of easy to identify crowns like dead trees, kanuka, tree ferns and flowering rata. An image guide was developed for the canopy stress symptoms based on RGB aerial images – see Appendix 7.3. The upper canopy trees of four permanent vegetation plots of Auckland University [25] were included in the analysis, after a field control of their position and an update of the stress symptom levels.

For the hyperspectral dataset, the reference crowns had to be re-evaluated to select the suitable crowns that were correctly positioned and not influenced by shadows or sensor anomalies. Some crowns had to be moved to the correct position on the hyperspectral image. Therefore, the crown set used for the hyperspectral analysis differs from the original reference crowns that were edited on the LiDAR height models.

The crown and pixel-based analysis require a high sub-meter spatial accuracy to match the LiDAR height models. Unfortunately, the survey points collected by Auckland Council did not match this accuracy and could not be directly included. However, this data was helpful in the survey preparation.

2.5.3 Software

Software	License	Use
ArcGIS 10.5	University of Trier	General GIS tasks, Spatial and 3D analysis
ATCOR-4	University of Canterbury, purchased with project money, four months evaluation license	Atmospheric correction of the hyperspectral image
ATCPro	University of Trier	Atmospheric correction of the hyperspectral image
eCognition	University of Trier	Crown segmentation
ENMAP toolbox	Open-source	Hyperspectral analysis, indices
ENVI	University of Trier	The main program for spectral analysis
ERDAS Imagine	University of Trier	Orthorectification of hyperspectral image
FLAASH	A three months evaluation license as a grant from Exelis, University of Canterbury	Atmospheric correction of the satellite images
LAStools	University of Trier	LiDAR preparation and analysis
MATLAB script	Dr Henning Buddenbaum, University of Trier	Destriping of hyperspectral data
PARGE	University of Trier	Geographic correction of the hyperspectral image
QGIS	Open-source	Raster analysis
R Studio	Open-source	Statistical tests and diagrams
WEKA	Open-source	Data mining, classification

Tableau 2: Field reference data

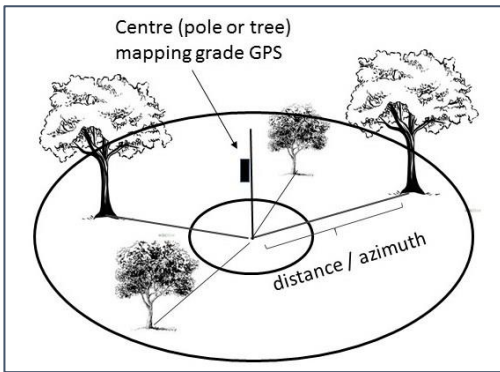


Figure: Design of a circular sample plot. The centre point is located by a mapping grade GNSS for 30minutes, while the trees are located via distance and bearing to the centre.



Photo: Centre station for circular sample plots with GPS, compass and vertex transponder.



Photo: Single tree mapping with a Bluetooth GPS on a hiking stick in the backpack, connected to QGIS maps on a tablet with aerial images and crown height model.

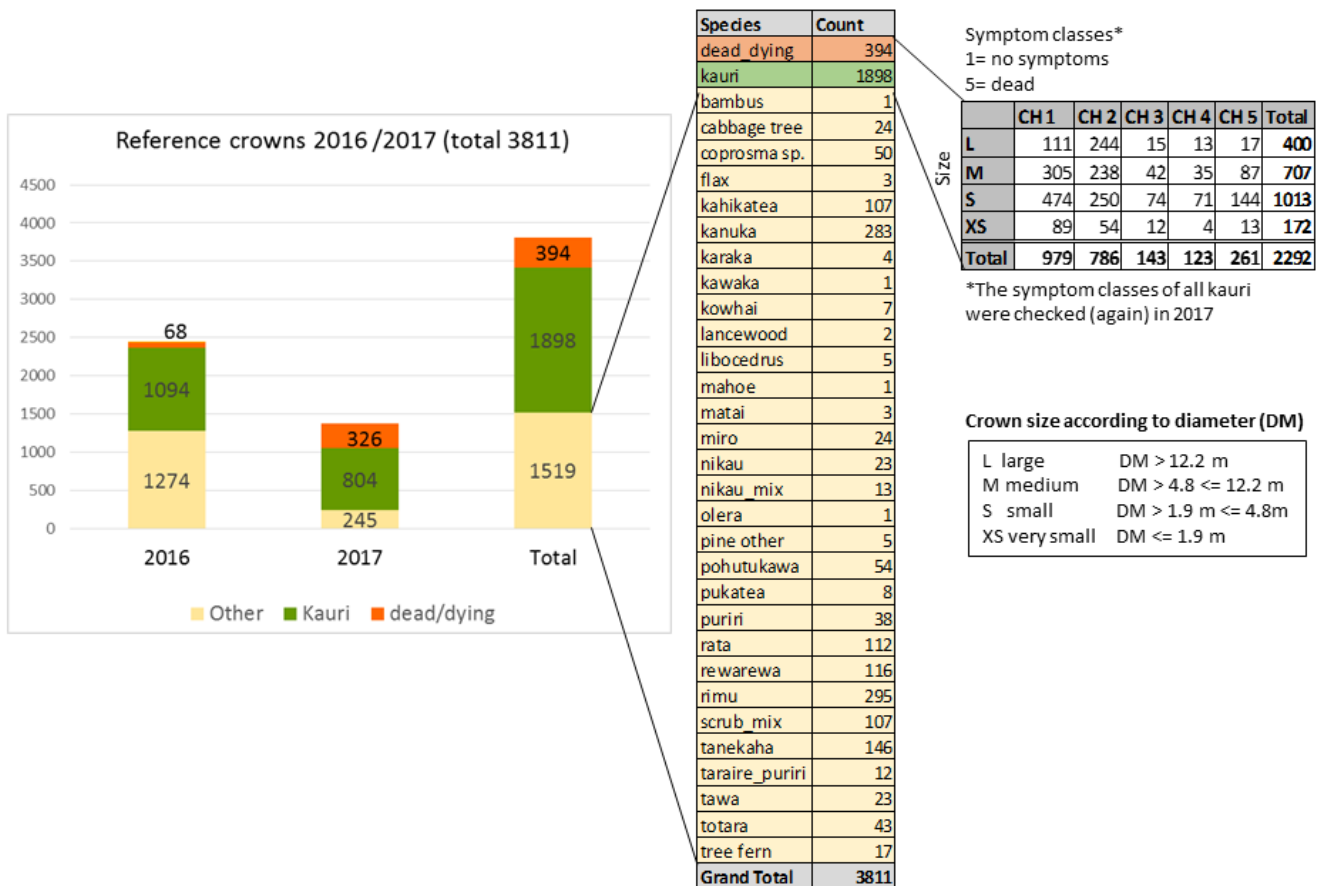


Figure: Total amount of reference crowns edited on the LiDAR crown height model. Overview over species, size- and symptom classes. However, the numbers of reference crowns that could be used for the analysis of the hyperspectral and satellite images are smaller. Crowns were removed that were outside the images or in the shadow of these images.

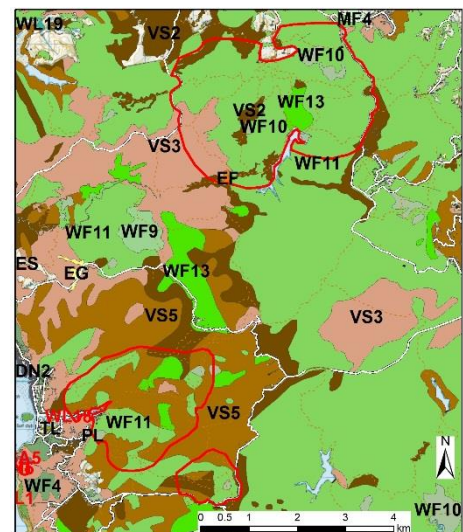
2.5.4 Phenological and ecological aspects of kauri and forest types in the study area

The leaves of kauri are broad needle-shaped, 2 to 5 cm long, with a smooth leathery surface. Younger leaves have a lanceolate shape and a green colour that often transitions into yellow to red [4]. Declining crowns show yellow to brown leaf colours— see also chapter 3.3. The leaves stick out from the branches in multiple directions and thereby creating an uneven foliage surface.

Young kauri, so-called "rickers", have a conical shape with dense foliage. Once the trees emerge over the main canopy, the crown spreads out to a dome shape, with a more open crown structure and foliage. The main branches in the mature trees emerge from a massive trunk and form an uneven, "bubbly" surface with smaller branches sticking out on the crown surface, which gives the profile of mature kauri a "shock-headed" appearance. The trees on the study sites grow up to ca. 40m tall and 30m wide. Taller height measurements were recorded in the LiDAR Crown Height Model (CHM), but they are most likely caused by an inaccurate terrain model or a large crown bending over a slope.

Most of the kauri trees in the three study areas occur in kauri-podocarp-broadleaved forest (see map to the right, code WF11) together with rimu, totara, miro, rata and tanekaha along the ridges and slopes, while kahikatea is more common in the lower areas and moist gullies. Only patches of mature kauri forests (WF10) are left in the Cascade area. Single kauri trees grow in the tawa-kohekohe-rewarewa-hinau-podocarp forest ecotype (WF13). Young kauri often grow under kanuka and manuka stands as nursery plants in kanuka scrub/forest (VS2) and broadleaved species scrub/forest (VS5). [14]

The shape and size of large kauri are unique compared to neighbouring tree species in the study areas. The conical shape of smaller ricker in contrary is quite similar to the shape of young rewarewa, tanekaha and rimu. With the hanging, scaled leaves, kahikatea has a smoother leaf structure than kauri (Tableau 3).



Map: Ecotypes in the study areas [14]




The needles of totara and matai, although smaller than kauri leaves, show a quite similar scattered foliage. The new kauri leaves in spring (around September to October) have a bright light-green colour. Flowering rata (red) and kanuka/manuka (white) are also standing out in spring. Unfortunately, the flowering is not synchronized and adds more variety to the forest appearance in spring.

While the large reference data set of kauri in different growth and symptom stages is representative for the Waitakere Ranges, some canopy species that are associated with kauri in other regions are underrepresented or missing, such as towai, kowhai, hard beech, taraire, pohutukawa, manao and yellow silver pine.






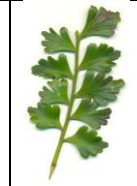








Tableau 3: Phenology of kauri and neighbouring tree species



Photos: Juvenile kauri leaves to the left and mature leaves in the middle in two colour variations from dark green to a bluish variant (Waitakere, January 2016). The leaves on the right photo are from a young tree under drought stress (Christchurch, December 2018).

Small (ricker)	Medium	Large
		
DM ≤4.8m	DM > 4.8m and ≤ 12.2m	DM > 12.2m

Photos: Kauri growth classes that were used in this study, depending on the crown diameter (DM). Photos: Waitakere Ranges, summer 2016.

Totara	Miro	Rimu	Kahikatea	Rata	Tanekaha	Rewarewa
						
						

Photos: Selection of common neighbouring tree species to kauri in NZ kauri forests (NZ Plant Conservation Network [26]).

3 Results

3.1 Spectral characteristics of kauri and separability from other species

Data preparation

The spectra of kauri with no visible stress symptom in the canopy (class 1) and of 21 other canopy species were extracted from the sunlit parts of the reference crowns on the hyperspectral image in ENVI. For the main analysis, all sunlit pixels were used to create the spectra. For test purposes, outliers from dead branches, epiphytes and neighbouring pixels were removed in ENVI's n-D Visualizer. The mean signatures and their separabilities were calculated in ENVI for both the original and the purified spectra. In the same way, the spectra of non-symptomatic kauri were extracted for different diameter size classes.

Results

Kauri spectra show distinctive characteristics in the far near-infrared (NIR) spectral region and comparably low values in the SWIR2 regions. The most distinctive features in the kauri spectrum are a steep ascend from 1000 nm to 1070 nm followed by a long descent to the absorption feature around 1215 nm. [1]

The spectra of non-symptomatic kauri crowns can be well separated from the spectra of the 21 other species (Jeffries-Matusita > 1.9 calculated in ENVI). The spectra of rewarewa, rimu, tanekaha, totara, miro and matai are most likely confused with kauri. After the removal of outliers and mixed pixels in ENVI's n-D Visualizer, the spectral separability of these species to kauri could be improved (see the table in Tableau 4, right column). [1]

The mean spectrum of small kauri crowns (diameter smaller than 3 m mean diameter) differs from the spectrum of larger crowns (Jeffries-Matusita value 1.84 [27], Transformed Divergence value of 1.95). This effect is most likely caused by the different foliage density and crown structure of smaller crowns and single mixed pixels in the smaller crowns that are influenced by the reflection of neighbouring species. The 1 m spatial resolution of the hyperspectral image is of limited suitability for objects with a diameter smaller than 3 m. These crowns are often misclassified due to the effect of mixed pixels and internal shadows in small stands.

Conclusion

- In addition to the visible bands, the kauri signature has distinctive characteristics in the far NIR region.
- The spectra of non-symptomatic kauri crowns can generally be well separated from crown spectra of the other canopy species analyzed in this study.
- The signatures of rewarewa, rimu, tanekaha totara and miro/matai are easiest confused with the kauri signature, especially for small crowns. After the removal of outliers and mixed pixels, they could be well separated.
- The spectra from small kauri crowns differ slightly from the spectra of larger kauri, due to a different foliage density and the influence of mixed pixels with neighbouring areas.

Tableau 4: Kauri spectral characteristics and separability from other canopy species

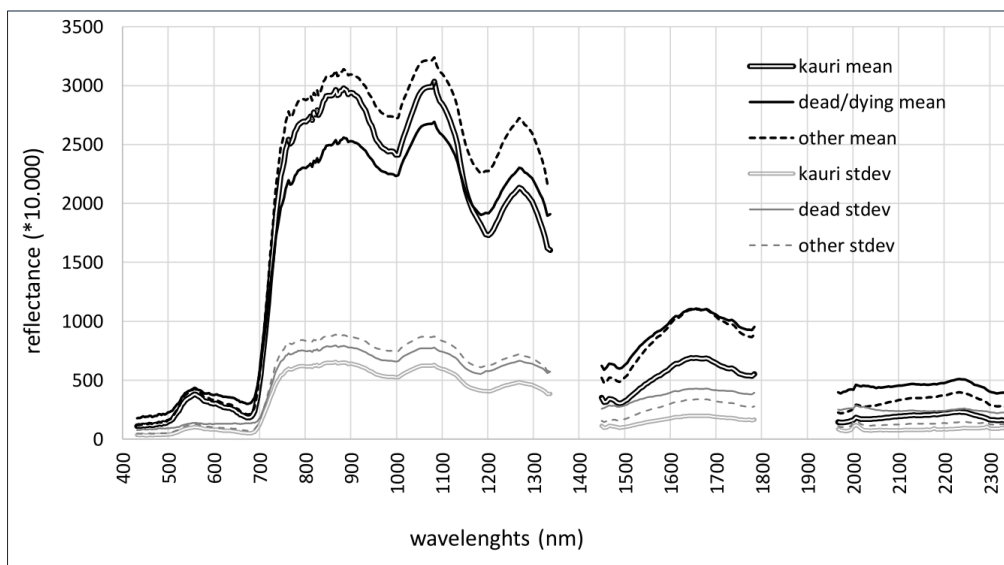


Figure: Mean spectra of the target classes "kauri", "dead/dying" and "other" with standard deviations (stdev) [1].

Species	All sunlit points	Selected points in nDViz
1 Kanukua	1.996	2.000
2 Cabbage	2.000	2.000
3 Flax	2.000	2.000
4 Karaka	2.000	2.000
5 Kahikatea	1.983	1.993
6 Kanuka flower	2.000	2.000
7 Kowhai	2.000	2.000
8 Libocedrus	1.999	2.000
9 Nikau	1.998	2.000
10 Pine	1.997	2.000
11 Pohutukawa	1.997	1.999
12 Scrub (Corposma etc.)	1.988	1.997
13 Puriri /Taraire	1.990	1.999
14 Rata	1.989	1.998
15 Rewarewa	1.968	1.995
16 Rimu	1.948	1.995
17 Tanekaha	1.860	1.992
18 Tawa	1.996	2.000
19 Totara	1.929	1.979
20 Miro/Matai	1.960	1.995
21 Tree Fern	2.000	2.000

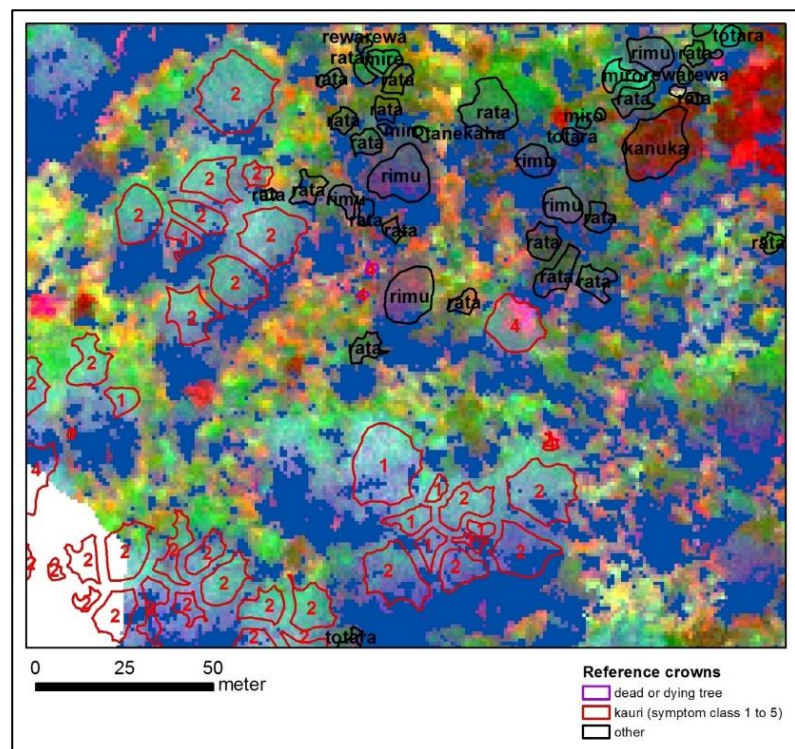


Table: Separability of kauri spectra from 21 trees spectra, calculated as Jeffries-Matusita value in ENVI. A value larger than 1.9 indicates that the signatures can be well separated. The left column marks the separability of all sunlit crown pixels; the values in the right column are based on a pixel set with removed outliers.

Map: Visualization of the hyperspectral image information based on an MNF compression of all 352 bands. Healthy kauri shows a characteristically light blue colour, declining kauri a pink colour. These colours are just for illustration purposes and say nothing about the spectral crown characteristics.

3.2 Kauri identification

The aim for this part of the analysis was to distinguish both kauri trees with no to medium visible crown symptoms and dead or dying trees from other species with no to medium stress symptoms. The dead and dying trees also include other species since these cannot be separated spectrally from dead and dying kauri. The resulting "kauri mask" can be used as the template area for long-term monitoring of stress symptoms in kauri canopy. For more details, see Meiforth et al. 2019 [1].

3.2.1 Kauri identification with selected indices from the hyperspectral sensor

Data preparation

The preparation of the hyperspectral image was carried out in 6 steps [1]:

Step 1: Destriping of the raw stripes with a MatLab script that was developed by the University of Trier

Step 2: Atmospheric correction by adapting an individual sensor model and correcting for the atmospheric conditions according to the variable terrain elevation with the software ATCOR 4

Step 3: Geographic correction in PARGE to correct for the GPS position, altitude, roll, pitch, heading and offset

Step 4: Polynomial orthorectification on the LiDAR crown height model (CHM) based on manually identified ground control points in ERDAS Imagine

Step 5: Create seamless mosaics in ArcGIS

Step 6: Post-processing in ENVI to create the finale mosaic and mask out no data pixels, define bad bands, wavelengths and bandwidths.

Reference data: Each reference crown in the hyperspectral image was checked. If it was not possible to locate it on the image or it was too influenced by shadows, the crown was either deleted or moved, to match the correct pixel position in the image. The crowns were then sorted into three classes: Kauri symptom class 1-3 (no to moderate symptoms), dead or dying trees (symptom class 4-5) and other canopy species. The symptom classes are further explained in chapter 3.3. Shadow areas were removed with a brightness threshold. Edge effects were reduced by removing an internal buffer to the edge with the size of 10% of the crown diameter.

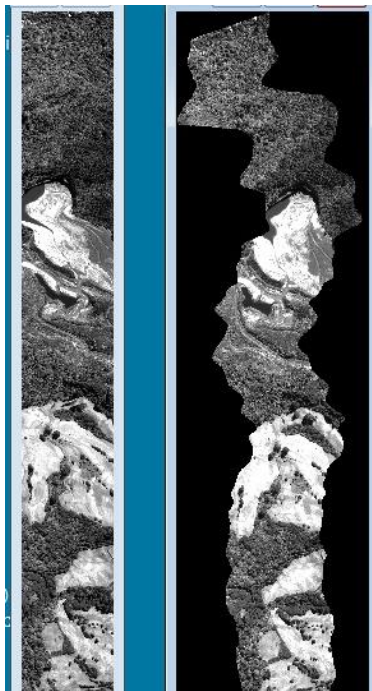
Bands: The 352 spectral bands were transformed with a Minimum Noise Fraction Transform (MNF transformation) in ENVI, and noisy bands were removed. In addition, 52 spectral indices were calculated in ENVI and the EnMap toolbox [28]. The values of each index were extracted for the reference pixels.

Analysis

The selection of the best indices to distinguish the three target classes was performed in the open-source data mining software WEKA. The results of several rankers and subset attribute selection methods were combined before attributes were excluded in an iterative process. The resulting attribute sets were tested with a Random Forest Classification and a 10-fold cross-validation until none of the resulting attributes could be removed without a significant drop in the classification accuracy.

Different classifiers were tested in a five-fold stratified random split in 10 repetitions for the accuracy assessment. The Random Forest classifier in the EnMAP toolbox was best suited to handle the very heterogenic three classes, compared to Maximum Likelihood and Support Vector Machine.

Tableau 5: Hyperspectral data preparation



Left: Correction for GPS position, altitude, roll, pitch, heading and offset in PARGE. Left stripe: before correction, right stripe: after correction



Right: Orthorectification with a polynomial model in ERDAS. Above: RGB band combination before and below after the orthorectification. The red polygons mark correctly positioned reference crowns on the LiDAR CHM.

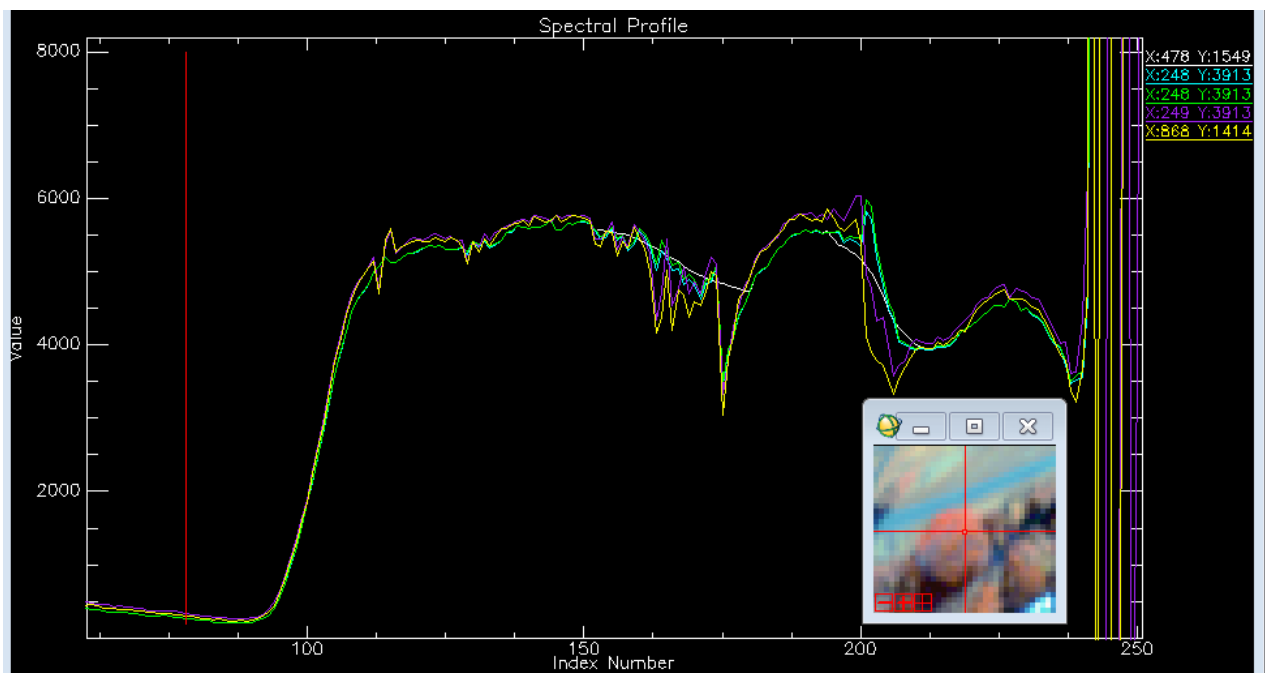


Diagram: Spectral profiles of a tree pixel after the atmospheric correction. Five different approaches for atmospheric correction are compared. For the analysis, the method based on an adapted sensor model and a variable water vapour on the 1130nm window was chosen (white – interpolated and cyan -not interpolated).

- White: Interpolated water vapour corrected on the 1130nm window, with sensor model adapted
- Cyan: No interpolation, water vapour corrected on 1130nm, with sensor model adapted
- Green: No interpolation, water vapour corrected on 940nm optimized band selection, with sensor model adapted
- Purple: Variable water vapour correction, no sensor model
- Yellow: Fixed water vapour (1.39mm), no sensor model

Results and interpretation

When all 352 hyperspectral bands were used in the form of 25 bands of an MNF transformation, a pixel-based overall accuracy of 96.2% (crown aggregated 91.8%) could be achieved to distinguish "kauri and dead and dying trees" from "other vegetation" for crowns larger 3 m diameter. [1]

As a result of the attribute selection, five spectral bands could be identified, which enable the distinction of kauri and dead/dying trees from other forest vegetation with a pixel-based accuracy of 93.8%. The crown-aggregated overall accuracy with 93%, is lower, because small crowns (< 3m diameter), that are more difficult to detect, weight more in a crown-aggregated analysis. The five selected multispectral bands cover both the visible range (VIS) in the 670 nm and 708 nm wavelengths, the first near-infrared range (NIR1) at 800nm and the far near-infrared range (NIR2) 1074 and 1209 nm. [1]

The 1 m pixel image is not suitable to detect kauri crowns smaller than 3 m mean crown diameter due to the effect of mixed pixels (see table below). In dense stands with small trees, shadows cause an additional problem for the classification. The main species that are incorrectly classified as kauri tend to have a similar "rough" foliage or needle-like leaves such as rimu, tanekaha, rewarewa, tōtara, miro and kawaka. Other species that are easily confused with small kauri have similar conical shapes in smaller growth stages such as tanekaha, rimu, kahikatea and rewarewa.

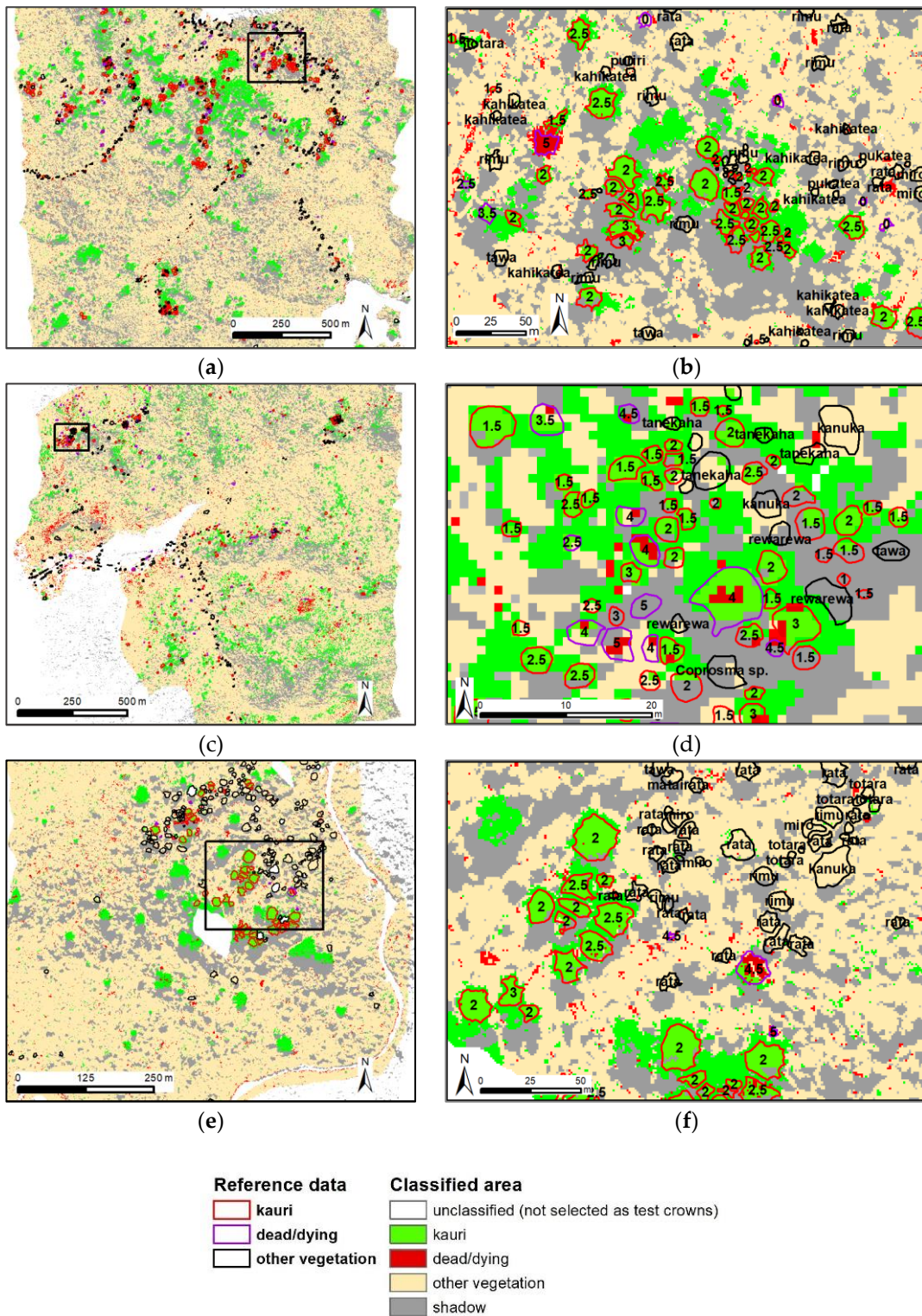
Conclusions

- With an overall pixel-based accuracy of 96.2% (crown aggregated 91.8%) on all hyperspectral bands, the kauri and dead/dying trees can well be distinguished from other forest vegetation.
- A selection of five spectral bands from the hyperspectral sensor in the visible to far NIR region performs well to distinguish the kauri and dead/dying trees from other forest vegetation (pixel-based accuracy 93.8%, crown aggregated 93.0%).
- The 1 m pixel size of the hyperspectral image causes problems with mixed pixels in crowns with a diameter size smaller than 3 meters. For the monitoring of small crowns, an image with a higher spatial resolution (<=0.5m) should be used. If a larger pixel size is necessary, the mapping unit for small crowns should be defined as homogenous stand segments.
- Kauri gets most easily confused with species with a spiky or "rough" foliage like rimu, tanekaha and totara. Moreover, species with similar conical shapes in smaller growth stages such as tanekaha, rimu, kahikatea and rewarewa get confused with small kauri.
- The geographic and atmospheric correction of the hyperspectral was very elaborate and required expert knowledge.

Table: Overall accuracies for a Random Forest classification for three classes (kauri <> dead/dying <> others) and two classes, with kauri and dead/dying aggregated in one class. The accuracies are given with standard deviations for a pixel-based, and a crown aggregated analysis. Pixel-based training and test pixels were randomly selected on all crowns on five bands (10 nm bandwidths) and a separated analysis for low and high stands.

	2 classes			3 classes			Users Accuracy			Producers Accuracy		
	all DM	>=3 m	< 3 m	all DM	>=3 m	< 3 m	kauri	dead	other	kauri	dead	other
Pixel-based	93.4 (0.1)	93.8 (0.1)	69.0 (2.1)	91.3 (0.1)	91.7 (0.1)	66.6 (2.0)	94.6 (0.2)	80.3 (0.7)	88.3 (0.3)	94.8 (0.2)	52.1 (1.4)	94.7 (0.3)
Crown-aggregated	89.7 (1.2)	93.0 (1.3)	72.6 (4.8)	87.3 (1.2)	90.8 (1.3)	68.3 (4.4)	94.0 (0.9)	75.0 (3.8)	84.4 (1.9)	87.6 (1.9)	74.4 (3.8)	91.2 (1.8)

Tableau 6: Kauri identification with five selected bands



Maps: Results of RF classification with a 5-fold stratified random split for the training and test data 10 repetitions. Overview (left) and detailed maps (right) for the Cascades (a, b), Maungaroa (c, d) and Kauri Grove area (e, f). The numbers indicate the stress symptom classes in kauri crowns (1 = non-symptomatic, 5 = dead). [1]

3.2.2 Combined optical and LiDAR data for kauri identification

The aim was to test the performance of optical datasets in combination with LiDAR data to distinguish kauri and dying trees from other canopy tree species in a crown-based analysis.

Data preparation

The reference crowns (total 1216) were located on both the LiDAR data and the sunlit areas of the optical data. Spectral indices were derived from three optical datasets:

- the 5 selected bands from the airborne hyperspectral sensor in the visible to far near-infrared (VNIR2);
- 4 bands of an airborne multispectral sensor (HiRAMS) and a 3-band red-green-blue (RGB) aerial image (HiRES) in the visible to first near-infrared range (VNIR1); and
- 8 multispectral bands of a WorldView-2 satellite image in the VNIR1 range.

Crown-based LiDAR attributes were calculated both on the original point cloud, spike-free digital surface and crown height models [29] and derived raster layers in LAStools, ArcGIS and QGIS/GRASS. The statistics are related to the shape and volume of the crown, measures of height, surface roughness, derived from the slope and textures in different directions, the crown density and coverage. The LiDAR attributes also include intensity values and thereby spectral information.

The eight multispectral bands of the WorldView-2 (WV2) image cover the VIS and first NIR areas up to 1040nm wavelengths (Tableau 7). The spatial resolution of the multispectral bands at nadir is 1.8m, and the black and white PAN channel has a nadir resolution of 0.45m. The image was corrected in four steps:

1. The multispectral and PAN images were orthorectified with the included Rational Polynomial Coefficients (RPCs) points on a 1m DTM.
2. The multispectral image was atmospherically corrected with FLAASH in ENVI
3. The 2m multispectral bands were pan-sharpened with a Gram-Schmidt Spectral sharpening in ENVI. An attempt with a Hyperspherical Color Sharpening (HCS) in ERDAS resulted in lower accuracy.
4. The resulting pan-sharpened image was orthorectified with ground control points in ERDAS Imagine to match the crown polygons. The mean control point error for the WV2 image in the three study areas was an RMSE of 0.87 m (X 0.57 m, Y 0.66 m).

For the WV2 image, 120 attribute layers were calculated in ENVI, the EnMAP toolbox and QGIS/GRASS from the original eight multispectral bands, including spectral indices, ratios, MNF and PC transformations, curvatures and textures. The attributes from the optical data were aggregated for each crown as mean and standard deviation for the spectral indices and in addition also as median, range and variance for the LiDAR data.

Analysis

The attribute selection for the three target classes "kauri", "dead/dying" and "other" was performed for each dataset in WEKA in a similar process as described above for the hyperspectral attribute selection. The accuracies for the different data combinations were analyzed in WEKA with a Random Forest classification in a 10-fold cross-validation.

Results and interpretation

LiDAR data alone resulted in an accuracy of 87.7% for the classification of the three target classes. The sensors with bands in the VNIR1 range performed lower with 83% accuracy for the HiRAMs and HiRES data and 82% for the satellite image¹ (Tableau 8).

A combination with LiDAR attributes improved the classification results significantly to 91% respective 90%. However, the 93% accuracy of the 5-band VNIR2 combination that includes the most characteristic spectral

¹ An earlier pixel-based WorldView-2 analysis for kauri identification with over 90.000 training pixels and 100.000 test pixels for all crown sizes, including crowns < 3m diameter, resulted in an accuracy of 80.25% for two classes (kauri/dead/dying <> other) and 79.03% for three classes (kauri <> dead/dying <> other).

features for kauri in the far near-infrared could not be improved with additional LiDAR attributes. A test with two stripes of data from the same LiDAR sensor that was used for the Northland flights (5.8 returns/m²) gave comparable results. The accuracies to distinguish the aggregated class "kauri and dead/dying" from "other canopy species" are about 1 to 2% higher than the analysis with three target classes.

Dead trees with a skeleton shape can be distinguished from dead trees with a dense canopy such as kanuka/manuka by a combination of the LiDAR intensity values with a raster variance attribute.

The requirement that the reference crowns had to match spatially with all datasets reduced the suitable amounts of small crown sizes for this analysis. An earlier analysis with a higher number of smaller crowns resulted in slightly lower accuracies².

Conclusion

LiDAR attributes can significantly enhance the identification of kauri and dead and dying trees with standard bands in the VNIR1 spectral range, given that the datasets are accurately spatially aligned and that the crowns are correctly segmented for a crown-based analysis. However, when the most characteristic spectral bands for kauri detection in the far near-infrared are available, additional LiDAR attributes do not enhance the accuracy. A test with the LiDAR data flown as part of the Northland data acquisition (Appendix 7.2) for a smaller area, gave comparable results.

Tableau 7: WorldView-2 satellite data

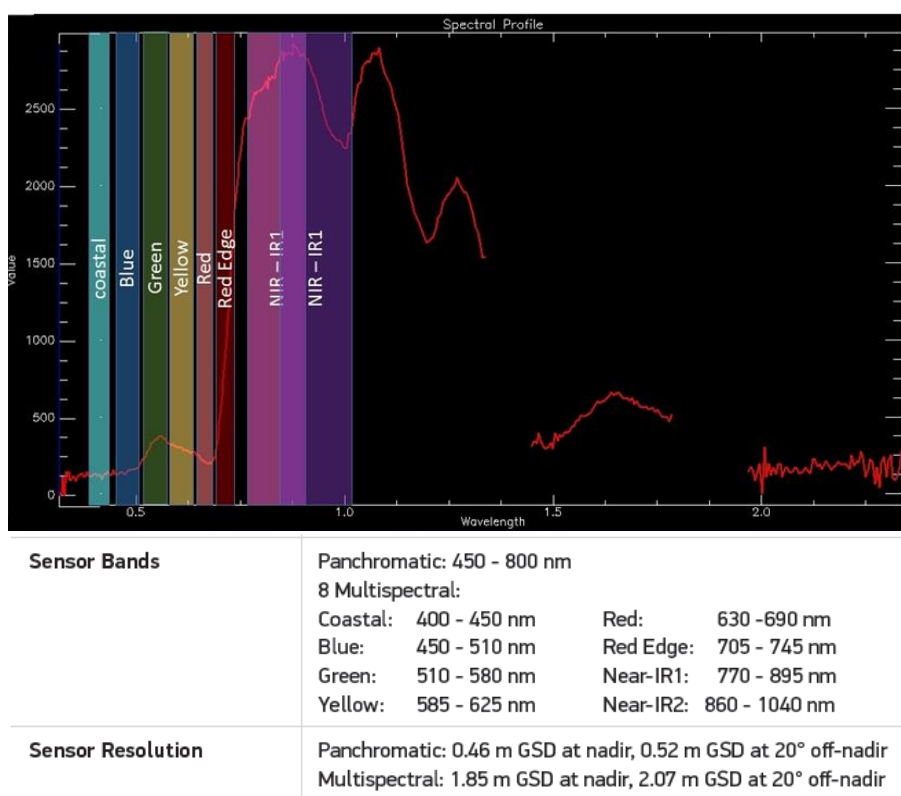
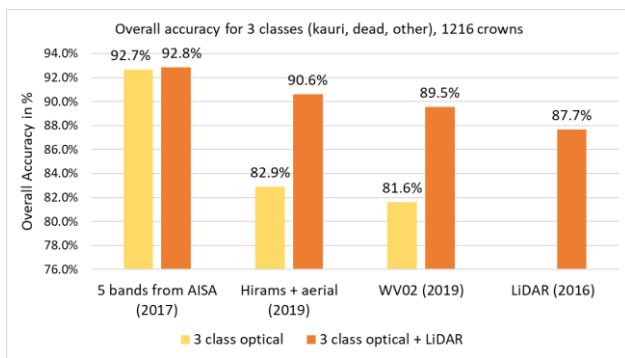


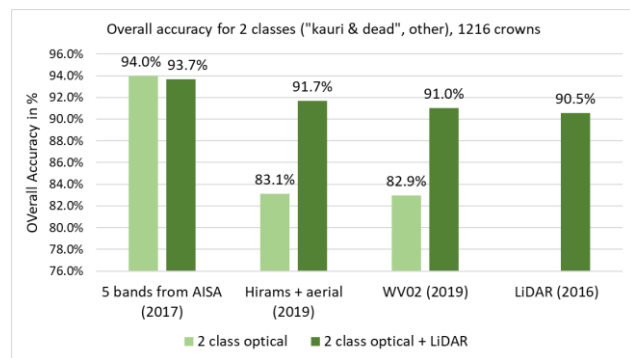
Figure: WorldView-2 – spectral bands and spatial resolution

² An earlier analysis only looked at the combination of the 5 bands (visible to far near-infrared) and an RGB image with LiDAR attributes to distinguish the three target classes with a total of 2271 reference crowns larger 3m diameter. Only LiDAR attributes resulted in an accuracy of 86.4%. Additional bands from an RGB aerial image enhanced the accuracy to 87.56%. The performance of the 5 bands could be enhanced from 90.04% with additional LiDAR data to 93.8%.

Tableau 8: Kauri identification: Optical & LiDAR data (crown-based)

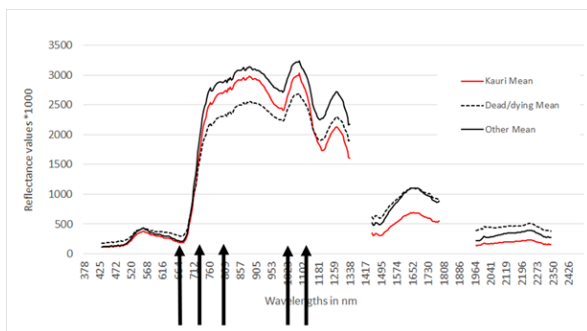


(a)

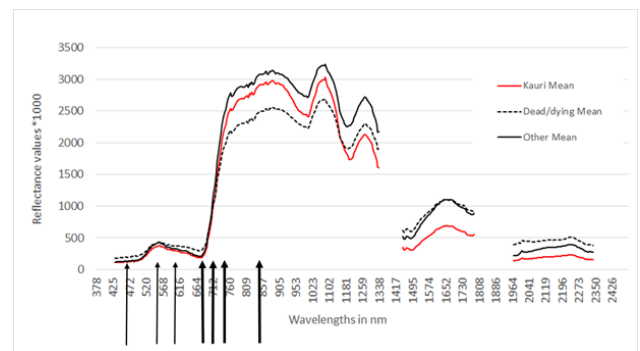


(b)

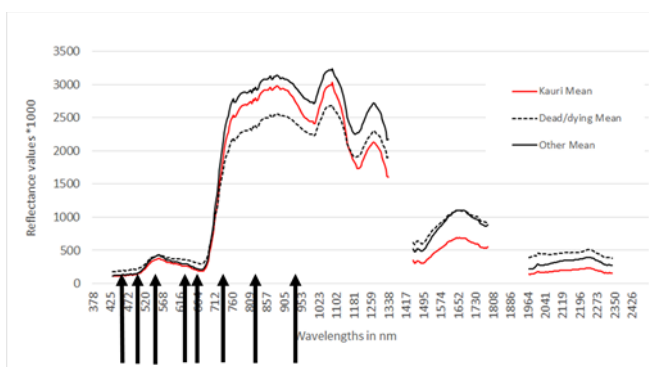
Figures: The diagrams show the accuracies of crown-based Random Forest classifications in WEKA with a 10-fold cross-validation on different optical datasets with and without additional LiDAR attributes. The analysis was performed for (a) three classes ("kauri", "dead/dying" and "other canopy species") and (b) 2 classes ("kauri and dead/dying", "other canopy species"). The optical datasets include the five selected bands from the hyperspectral sensor in 10 nm bandwidth, 4-bands from a Hiram's multispectral sensor with 3-band aerial image (HiRES) and the 8-band WorldView-2 satellite data.



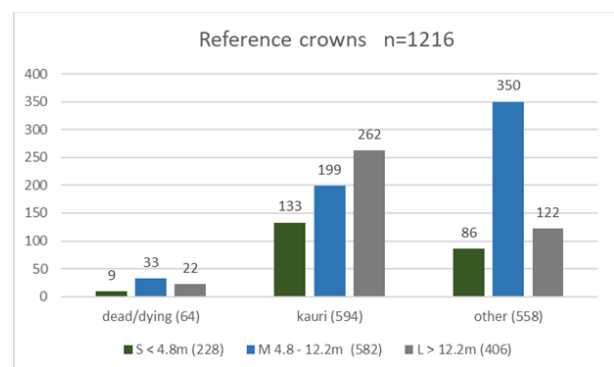
(a) Five multispectral bands selected from the hyperspectral sensor



(b) Three red-green-blue aerial bands and four bands from the Hiram's multispectral sensor



(c) WorldView-2 satellite image, eight multispectral bands



(d) Overview size and target classes for the reference crowns used in this analysis.

Figures: Positions of spectral bands from the three optical datasets used in this analysis (a) to (c) in relation to the mean spectra of kauri (red), dead and dying trees (stippled) and other canopy species (black). The diagram (d) gives an overview of the number of reference crowns per target class and size class from small to large.

3.3 Detect symptoms of stress in the canopy

3.3.1 Physiological processes and visible symptoms in infected kauri canopies

The kauri dieback disease is caused by the soil-borne pathogen "*Phytophthora agathidicida*" [30]. It enters the kauri roots, spreads in the tissue and blocks the transport of nutrients and water to the canopy [7]. The first effects on the leaf level is a decrease in the leaf water content and photosynthetic activity which eventually leads to degradation and withdrawal of the chlorophyll content. At this stage, the first visible symptoms in the canopy are yellowing and browning of leaves. In the next stage, the tree will drop the leaves, the canopy loses its overall biomass, internal crown shadows increase, and bare branch material becomes more visible, starting with the small top branches. Eventually, the tree drops all the leaves and later also branches until only a skeleton is left. These symptoms can also have other causes such as drought stress or other pathogens. The remote sensing analysis is only able to detect symptoms that are correlated with the occurrence of the disease, but it cannot prove the disease itself.

3.3.2 Spectral characteristics of stress symptoms in kauri canopies

Data preparation

The recorded attributes in the field included the stem position, the cardinal crown spread, the stem diameter at breast height [31], the canopy base height, an estimated crown density and a foliage coverage [32]. Optical characteristics like the yellowing of leaves and anomalies like epiphytes or double stems were noted, and each recorded kauri was documented with a canopy photo. Dead branches were documented in six percentage classes. Stress symptoms in the canopy were assessed in 5 symptoms levels from 1 = "non-symptomatic" to 5 = "dead", corresponding to the classification scheme of Auckland Council. The final assessment of stress symptoms was based on an evaluation of both the fieldwork and visible stress symptoms on RGB aerial images from 2016 and 2017. In high and dense stands the aerial images from 2016 and 2017, were better suited as a reference for the canopy symptoms than the ground field data. An assessment scheme for the interpretation of visible stress symptoms on RGB aerial images in five symptom levels was developed (see Appendix 7.3), to secure an objective and coherent assessment. It was applied equally to kauri crowns of all size classes without any interpretation of their health state.

The spectra of the sunlit part of the crowns in different symptom stages were extracted from the hyperspectral image in ENVI. For this analysis, only crowns from kauri and dead/dying trees larger 3 m crown diameter were used.

Results

The spectral signatures of declining kauri show the expected features of stress in vegetation [2]:

- Higher blue and red reflection, lower "green peak" due to reduced chlorophyll absorption
- Lower reflection in the NIR region due to reduced leave biomass
- Lower water absorption "valleys" due to a higher amount of dry matter and a loss of leaf water content. (There was still a lot of water absorption on the dead trees because the forest was moist during the acquisition and the spectra include green undergrowth.)
- Higher reflection in the SWIR 1 and 2 caused by higher amounts of cellulose, lignin and plant litter

The stress symptom levels need to be interpreted to translate them into an assessment of tree health. This interpretation needs to consider the size of the crown, the location, e.g. the proximity to infected trees, the growing conditions, e.g. the depths and moisture conditions of the soil or the exposure to sea salt and seasonal aspects like the influence of a drought. Smaller kauri crowns show different stress symptoms than larger crowns [2]. A small patch of a dead branch in a small tree can already be a severe health risk when it is caused by a dying top branch. In contrast, the larger kauri crowns show a certain amount of branch material even when they are still healthy. The first symptom classes indicates, therefore, a more severe health state for a smaller tree than for a larger tree crown.

Conclusion

- Declining kauri show characteristic stress features in both the VIS, NIR and SWIR regions of the spectra.
- A stressed kauri loses its characteristic kauri features and will be easier confused with other species.
- For most dead and dying crowns, it is not possible to identify if it is a kauri tree with optical data unless there is healthy foliage left.
- The spectral response in small kauri for different stress levels differs from the response in large crowns.
- High-resolution aerial images are better suited as a reference for the assessment of canopy symptom in dense stands with high trees than ground-truthing.
- The stress symptom levels detected by remote sensing need to be interpreted to translate them into an assessment of tree health.

Tableau 9: Stress symptoms in the kauri spectra

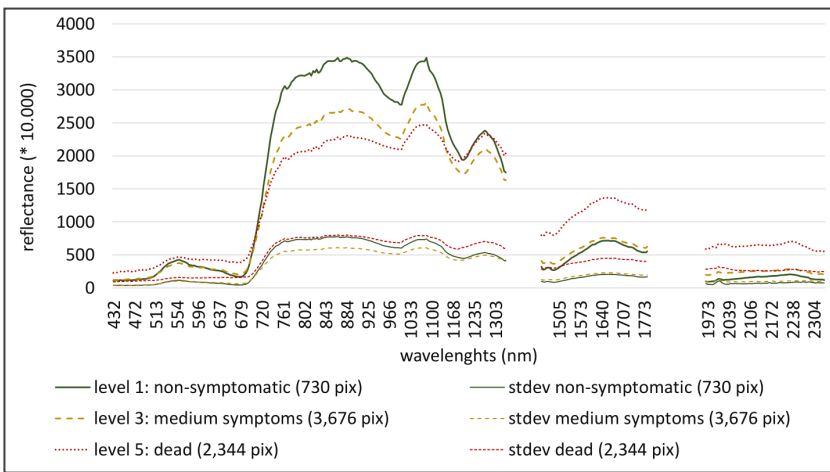
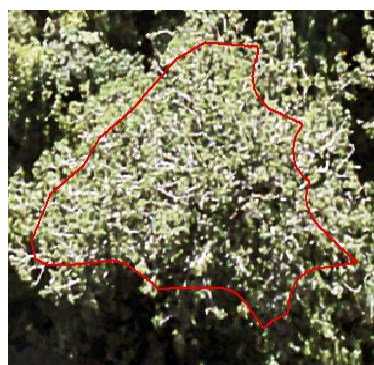


Figure to the left: Mean spectra (bold signatures) and standard deviation (stdev, thin signatures) of kauri in three symptom levels: Non-symptomatic (level 1, green), medium symptoms (level 3, orange) and dead trees (level 5, red). The number of pixels (pix) for the different levels is given in parentheses. [2]

Green: No to slight symptoms (level 1 -2)



Orange: Medium symptoms (level 3)



Red: Dead or dying (level 4 - 5)



Photos: Aerial images (2017) of large kauri crowns in different stages of stress symptoms (see assessment scheme in Appendix 7.3).

3.3.3 Detection of stress symptoms with selected vegetation indices from the hyperspectral image

The aim of this analysis was to develop a method to describe canopy stress symptoms of kauri crowns based on vegetation indices from selected bands of the hyperspectral image. Vegetation indices are combinations of spectral bands that are sensitive to specific spectral plant properties. For more details, see Meiforth et al. 2020a [2].

Data preparation and analysis

For the detection of stress symptoms, mean crown values were calculated on an initial selection of 95 spectral indices from the hyperspectral image. The sunlit parts of the crowns were defined with a brightness layer. Only crowns larger 3 m diameter were included for the analysis based to avoid mixed pixels on the image with a 1 m pixel size. These values were then combined with the crown-based symptom levels (chapter 3.3.2). The index selection was carried out in WEKA according to the method described in chapter 3.2.1. The crown-based analysis was performed as a Random Forest regression, which outperformed other regression algorithms [2].

Results of a crown-based analysis

Five indices on six bands in the visible to near-infrared region (450–970 nm) achieved a correlation of 0.93 with a Random Forest regression for the description of five stress symptom levels from non-symptomatic to dead. A stratified approach with individual models for pre-segmented low and high forest stands improved the overall performance. [2]

The selected indices are indicators of leaf pigments and photosynthetic activity (Normalized Difference VI–Aparicio, NDVI-A; Gitelson and Merzlyak Index 2, GM2 and a modified Ratio VI, mRVI) and canopy water content (Water Band Index, WBI) (see Tableau 10). The Normalized Difference Vegetation Index (NDVI-A) in the near-infrared/red spectral range was identified as the most important band combination to describe the full range of stress responses. In the more advanced stages, the loss of foliage and branch material causes structural changes and a further loss of canopy water, which is captured in the selected WBI. Pigment-sensitive indices with bands in the green, red and red-edge (GM2, mRVI) spectral ranges are more important for describing first stress symptoms and stress responses in smaller trees with denser foliage. [2]

On the full spectral range, additional indices were selected, which are sensitive to leaf water content (Leaf Water Vegetation Index), leaf nitrogen (Normalized Difference Nitrogen Index) and cellulose / dry matter (Short-wave Infrared Green Vegetation Index). They enhanced the correlation slightly to 0.94. However, these bands are located in spectral regions that are usually not captured by standard airborne multispectral sensors. For more information on these indices, see [2].

The same five multispectral bands that were already selected for the kauri detection also performed well for stress detection, with an overall correlation of 0.93 for five stress levels. The combination can be further improved for small crowns by adding a band in the green spectral range. However, this combination is adapted to the characteristic spectral features of kauri with bands in the far near-infrared and should be tested before using it for stress analysis in other tree species. [2]

This method requires a prior segmentation of crown polygons. So far, it was conducted on the reference crowns. A combination of automatically selected crown polygons based on the LiDAR data might result in a lower accuracy.

First results of a pixel-based analysis

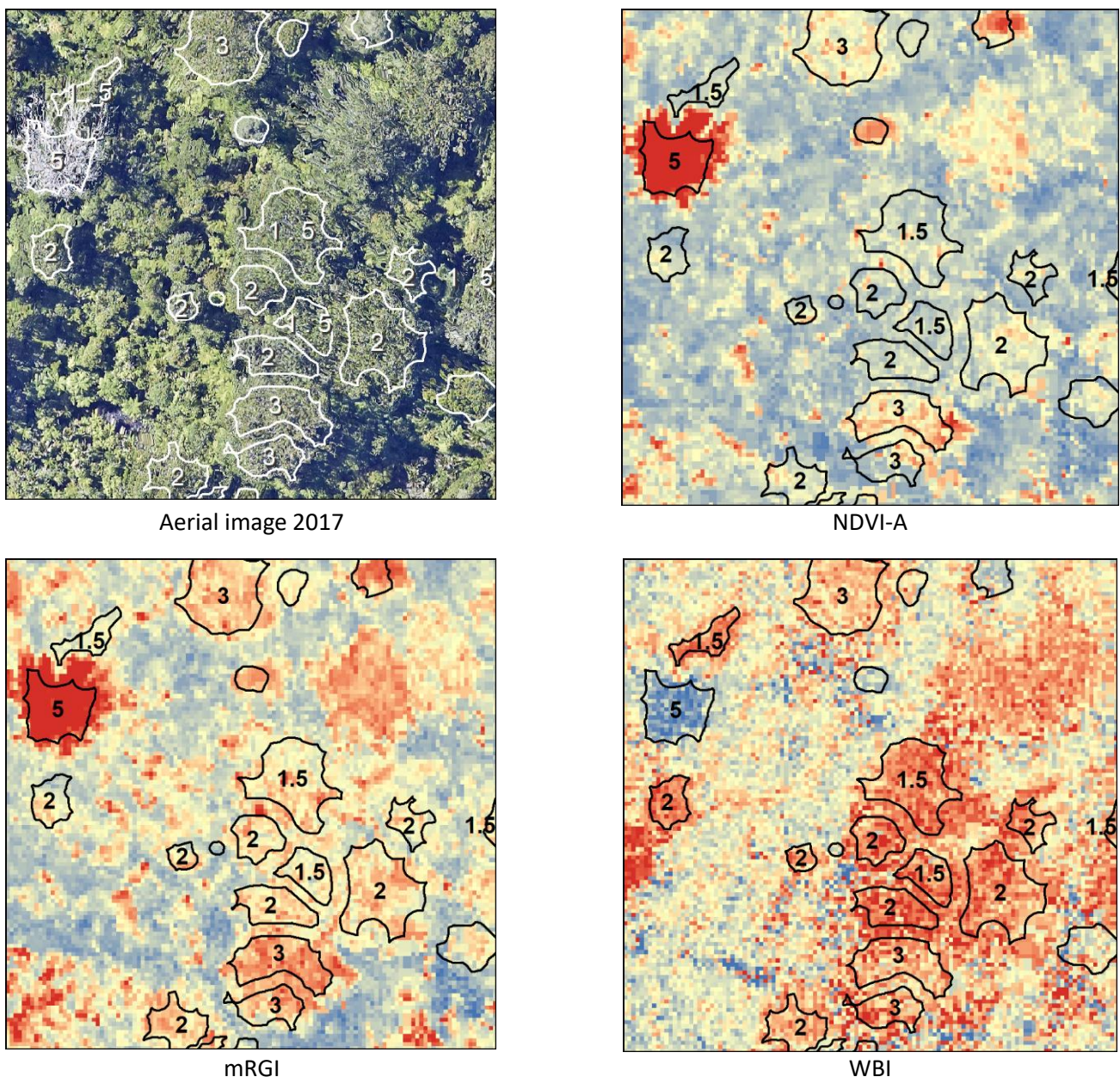
The use of the selected indices in a pixel-based analysis showed a good match compared to stress symptom patterns on aerial imagery. A first test of the pixel-based approach with a Random Forest regression on all crown sizes (including <3 m diameter) and bands in the full spectral range resulted in a correlation coefficient of 0.89 in a 10-fold cross-validation. A crown-based aggregation of the results could enhance the correlation to 0.91 for all crowns and 0.93 for crowns with a diameter larger 3 m. However, the pixel-based

approach should be further tested for the selected bands in the visible to NIR1 spectrum, which are easier to implement.

Conclusion

- For a 1 m pixel size in the image, the minimum recommended crown diameter is 3 m for the stress detection. Smaller tree crowns should be analyzed in homogenous stand units, or with a optical data in a higher spatial resolution.
- The best correlation to the symptom classes can be achieved with indices on the full spectral range, with a correlation coefficient of 0.94 in a crown-based Random Forest regression.
- With six standard multispectral bands in the VNIR1 spectral range, a correlation of 0.93 can be achieved.
- The five multispectral bands that were selected for the kauri identification result in a crown-based correlation of 0.93. An additional green band and a test for the use in other species is recommended.
- A stratification into different crown sizes improves the results. This can be done by a separated analysis of crowns in low and high forest stands, or in separated crown size classes.
- A crown-based analysis achieves higher correlations than a pixel-based analysis. However, it requires a prior crown segmentation, which introduces additional errors. The pixel-based approach should be further tested.

Tableau 10: Detection of stress symptoms with selected vegetation indices

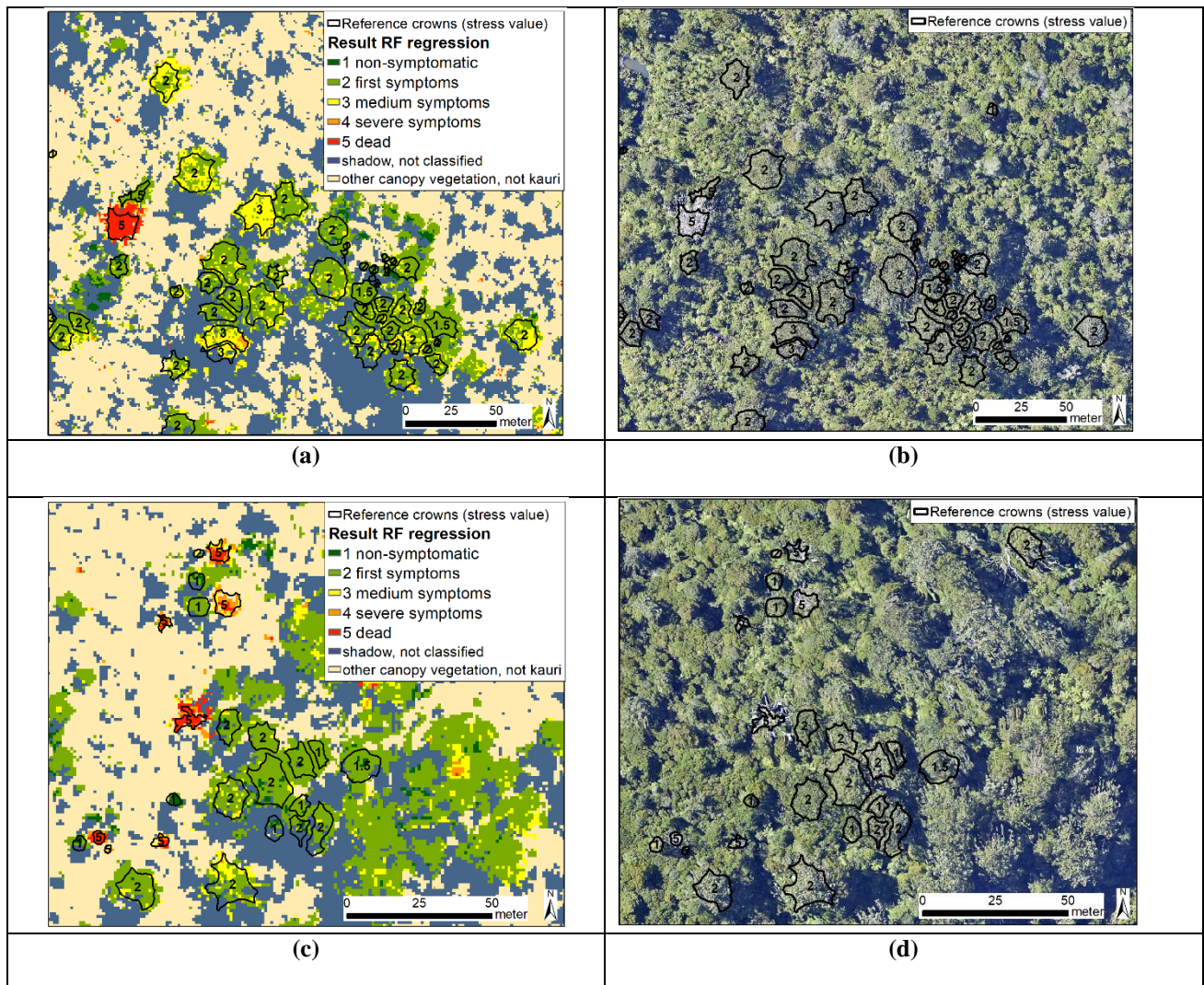


Figures: Aerial image and selected vegetation indices (description see table below; red=high values, blue =low values) in the visible to NIR1 spectral range with crown polygons and stress symptom classes (1=no symptoms to 5=dead).

Table: Selected Vegetation indices (VI) for the analysis of stress symptoms in kauri crowns in the visible to near-infrared bands (VNIR1). An "m" indicates that wavelengths had been slightly modified compared to the cited literature.

Index Abbr. ¹	Equation	Source	Name, Association
mRGI	= 685/550 (<i>original: 690</i>)	[33]	Red-Green Pigment Index (leaf pigments)
mNDVI-A	= (900 - 685)/(900 + 685) (<i>original: 680</i>)	[34]	Normalized Difference VI–Aparicio (broadband greenness)
GM2	= 750/700	[35]	Gitelson and Merzlyak Index 2 (chlorophyll)
mRVI	= 750/680 (<i>original: 745, 645</i>)	[36]	Ratio VI (chlorophyll content)
WBI	= 900/970	[37]	Water Band Index (canopy water)

Tableau 10 (continued): Detection of stress symptoms with selected vegetation indices



Figures: Resulting maps (a, c) and corresponding RGB aerial images (b, d) (2016) [38][37] of a pixel-based application of the 6-band VNIR1 index combination for two forest stands with marked reference crowns and their reference symptom class values. The analysis was carried out as a Random Forest regression in the ENMAP toolbox [28] on selected indices raster's for the full spectral range.

3.3.4 Detection of stress symptoms with WorldView-2 satellite data

The aim of this analysis was to test the suitability of WorldView-2 satellite data for stress detection in kauri crowns. For more details, see Meiforth et al. 2020b [3].

Data preparation

The analysis is based on a selection of 1089 crown polygons of kauri and dead/dying trees on the WorldView-2 image (WV2) with more than 50% sunlit area. The crown polygons were manually edited on the LiDAR crown height model. The stress symptoms assessment was based on fieldwork and an interpretation of aerial images, according to a method described in chapter 3.3.2 and Appendix 7.3 [2]. For a more detailed evaluation of the first stress symptoms, the stress levels 1 to 3 were refined in half-steps.

Analysis

Spectral (43) and textural (111) attributes were calculated as raster on the eight pan-sharpened multispectral WV2 bands with the band math tool in ENVI. For the crown-based analysis, the mean and standard deviation of each raster was calculated on the sunlit part of the crown polygons. The maximum crown height value from the LiDAR data was included in the analysis to allow for a size stratification. The attribute selection was performed in the software WEKA according to the procedure described in chapter 3.2.1, [3]. The analysis is crown-based with a Random Forest regression.

Results of a crown-based analysis

A size of 4 m mean diameter was defined as the recommended minimum crown size for the use of the WV2 image for stress detection, to avoid mixed pixels and to identify dying top branches in small crowns. A selection of eight WV2 attributes resulted in a correlation of 0.89 (Tableau 11).

The most important attributes are a combination of red/NIR1 bands in a Normalized Vegetation Index (NDVI_75), followed by a ratio of the red and green bands (Red-Green Ratio Index (RGRI)) and the standard deviation of the first band of an MNF transformation. Mean crown values of a Green NDVI (gNDVI) with red-edge and green bands, the red-edge band, and a brightness layer were also selected. Further attributes include the mean value of a seven-pixel kernel of the PAN band and the range of a three-pixel kernel on the NIR1 band.

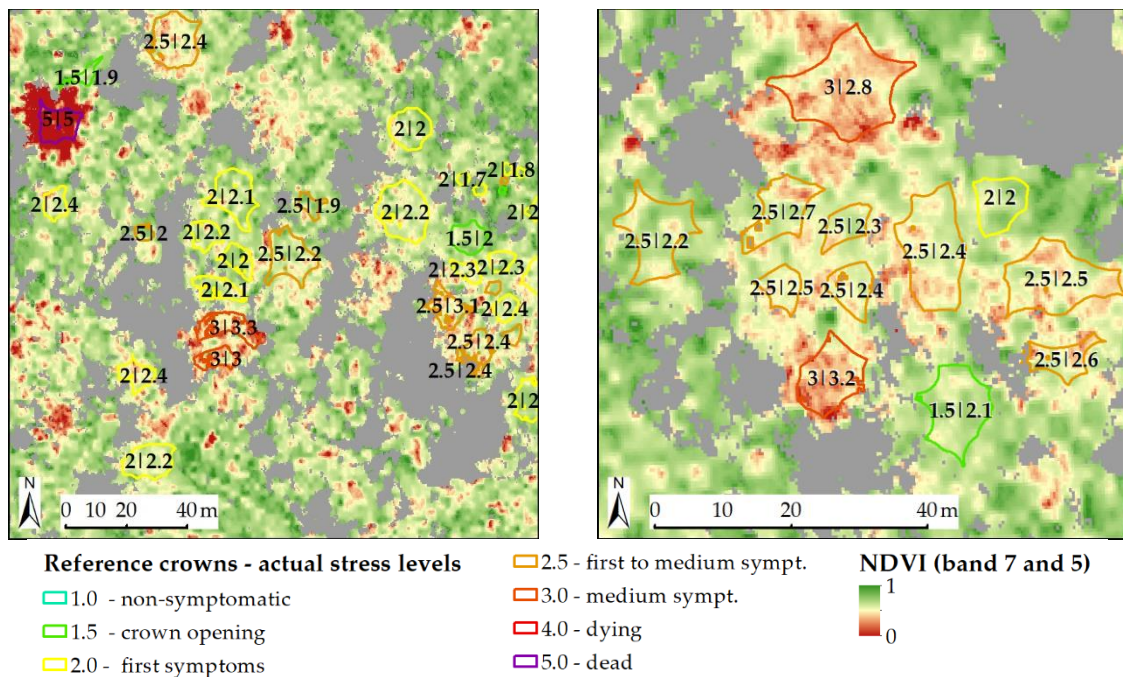
First test results of a pixel-based analysis

In an earlier analysis for all crown sizes, a pixel-based approach resulted in a Random Forest correlation of 0.85 with 15 selected attributes. The use of a pixel-based analysis with WV2 data should be further tested. A challenge was the generation of defined training pixels with the crown-based reference data since declining crowns often show a heterogeneous symptom pattern. The pixel-based results might be improved by applying a minimum crown size, the generation of training data from mean crown values or pixels from crowns with homogenous stress symptoms throughout the full crown polygon.

Conclusion

- The WorldView-2 image is suited to monitor changes in stress symptoms in the kauri canopy with a crown-based correlation coefficient of 0.89 in a Random Forest Regression for crowns of at least 4 m diameter.
- The minimum recommended crown diameter is 4 m for the use of the 1.8 m resolution in the WorldView-2 multispectral bands, even after they are pan-sharpened to 0.5m. Smaller crowns should be analyzed in homogenous stand segments.
- This method requires a prior segmentation of crown polygons. So far, it was conducted on the manually edited reference crowns. A combination of automatically selected crown polygons based on the LiDAR data might result in lower accuracy. A pixel-based analysis should be further tested.

Tableau 11: Detection of stress symptoms with a WorldView-2 image



Maps: Reference crowns in two forest stands in the Cascade area. The labels indicate the actual stress levels (left number) and the predicted stress levels (right number) on an NDVI background raster (bands 5, 7). The predicted values are based on five stress levels with refined first symptom stages and WV2 attributes according to the table below.

Table. Selection of WV2 attributes and their importance for a description of the seven-level reference scheme. The maximum crown height value was added for crown stratification. The attribute importance (imp.) for the RF regression was calculated as the average impurity decrease and converted to the percentage.

Abbr.	Att. Imp. %	Correlation	Crown Statistic	Description	Algorithm	Source
NDVI	32.5	-0.83	mean	Normalized Difference Vegetation Index	$(b7 - b5)/(b7 + b5)^1$	[39,40]
RGRI	25.0	0.79	mean	Red-Green Ratio Index	$b5/b3^1$	[41]
MNF1	12.6	0.68	st. dev.	1st band of a minimum noise fraction (MNF) transformation		[42]
NDVIg	9.2	0.70	mean	green NDVI	$(b6 - b3)/(b6 + b3)^1$	[43]
b7O3rg	4.3	-0.05	mean	range of a 3×3 kernel of band 7		[44]
Bright	3.9	-0.14	mean	brightness band	$(b2 + b3 + b5 + b7)/4_1$	[45]
b06	3.7	-0.15	mean	mean of band 6 (red-edge)		
PO7mn	2.8	-0.21	st. dev.	mean of a 7×7 kernel of the panchromatic (PAN) band		[44]
CHM	5.8	-0.18	max	maximum height on a CHM raster (1 m freeze distance)		[46]

¹ The variables marked with "b" indicate the band numbers of the WV2 image.

3.3.5 Improving optical stress analysis with LiDAR data

The aim of this analysis was to if additional LiDAR data can improve stress detection with optical data in kauri crowns.

Data preparation

The use of LiDAR data to improve canopy stress detection with optical data for kauri and dead/dying trees was tested in two setups:

- with five selected bands from the hyperspectral sensor (1 m pixel resolution) on the full spectral range ("multispectral bands") on 1280 crowns with a minimum crown size of 3 m.
- and with attributes from the WorldView-2 image (1.8 m original pixel resolution, pan-sharpened to 1.8 m) for 1089 crowns with a minimum crown size of 3 m and 895 crowns with a minimum crown size of 4 m.

The number of crowns differs for both setups, because of different diameter sizes, different area coverage and shadow affected areas for the optical data. To account for the fact that the LiDAR data was acquired in 2016, one season before the hyperspectral and WV2 image, the aerial images from both years (2016 and 2017) were compared. Crowns that showed visible changes or where the status of the crown could not be identified on both aerial images were removed.

Analysis and results

The analysis was carried out crown-based in WEKA as a Random Forest regression for symptom levels from 1 = non-symptomatic to 5 = dead. Compared to the performance of five selected bands from the hyperspectral sensor on the full spectral range, additional LiDAR data only slightly improved the correlation in a stress detection from 0.940 to 0.948 for crowns larger 3 m diameter.

In combination with the WV2 attributes, the additional LiDAR data improved the correlation from 0.89 to 0.92 (RMSE from 0.48 to 0.43). The most important attributes for a combination of LiDAR and WV2 data are an NDVI on the red/NIR1 bands, followed by a ratio between the maximum height and the 50 percentile crown height (R_{max_P50}) and the average intensity values. The standard deviation of the first MNF band was also selected with high importance amongst other spatial attributes for crowns with a diameter larger than 4 m. Both the identification of dead and dying trees, as well as the detection of first stress symptoms, improved with additional LiDAR attributes. For more details about the selected attributes, see Meiforth et al. 2020b [3].

Conclusion

- For optical data with a spatial resolution larger than 1 m pixel size, like WorldView-2 satellite data, additional LiDAR data improves the stress detection significantly in a crown-based analysis, especially for small crowns. However, for the stress assessment, the datasets need to be available for the same season.
- For optical data with a spatial resolution of 1 m or smaller, additional LiDAR data does not make much difference in the stress detection. If it is available for the same season, it can be added, but the results do not justify the much more elaborate process of a prior crown segmentation and a new data acquisition.

Tableau 12: Improving optical stress analysis with LiDAR data

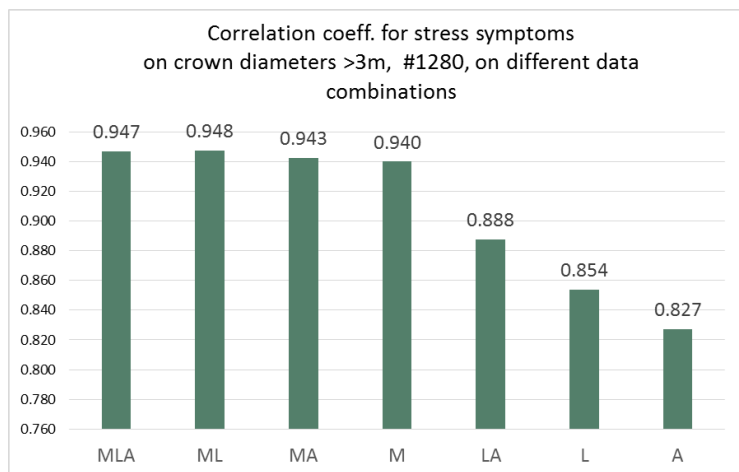
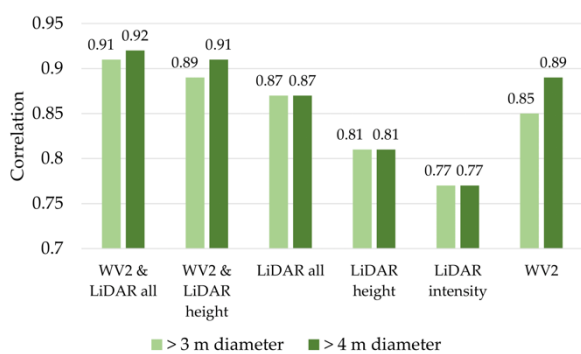
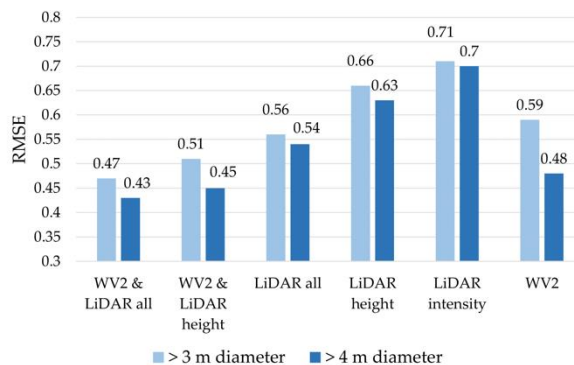


Figure: Correlation coefficient for the detection of stress symptoms in five levels for different data combinations (M= 5 multispectral bands, L = LiDAR, A= Aerial). The analysis is based on a Random Forest Regression for 1280 crowns larger 3 m diameter. The multispectral bands cover the full spectral range.



(a)



(b)

Figure: Correlations (a) and RMSE (b) of WV2 and LiDAR attributes for a Random Forest (RF) regression on refined stress symptom levels from 1 to 5 (1 – 1.5 – 2 – 2.5 -3 - 4 -5). The performance was tested for crowns with a mean diameter larger than 3 m (light colour, total 1089) and larger than 4 m (dark colour, total 895). The RF regression was carried out in 1000 repetitions for a random 3-fold split with a tree depth of eight.

3.4 Automatic stand and crown segmentation

3.4.1 Stand segmentation

The aim of the stand segmentation was to identify structurally homogenous forest stands. The stand segments were used to stratify the reference crowns for kauri and stress detection. They also enhanced the automatic crown segmentation by separating areas with small crowns from the areas with medium and large crown diameters. The stand units can also serve as reporting units to aggregate the results of a pixel-based classification.

Data preparation and analysis

Spike-free LiDAR crown height and surface models were developed with LAStools. Versions with and without a low pass filter were prepared. The blue band of the aerial image improved the segmentation. Based on the LiDAR data and the aerial images from 2016, a multiresolution segmentation in eCognition was developed, to segment different stand situations automatically. The largest unit of the segmentation matches the largest kauri crown diameters of ca. 35 m in the study area.

The analysis is structured in four steps; the resulting maps of step 1 and 3 are displayed in Tableau 13:

1. Sinks: In a first step, sinks are masked out – see blue coloured areas on the map.
2. Segmentation: In a second step, the unclassified areas are segmented with a scale value of 120 on a 0.15cm unit, which is suitable to cover the widest crowns in the area.
3. Classification: In the third step, these segments were classified and reshaped in three different stand situations, small, medium and large to facilitate the crown segmentation. The main attributes for the classification are the height, the skewness, border contrast, contrast, homogeneity and standard deviation.
To facilitate the pixel-based kauri and stress detection, only two stand situations, low and high, were distinguished, with a mean height threshold of 21 m.
4. Adjustment: The polygons are dissolved and adjusted so that small "sliders" are merged into adjacent larger stands.

Results

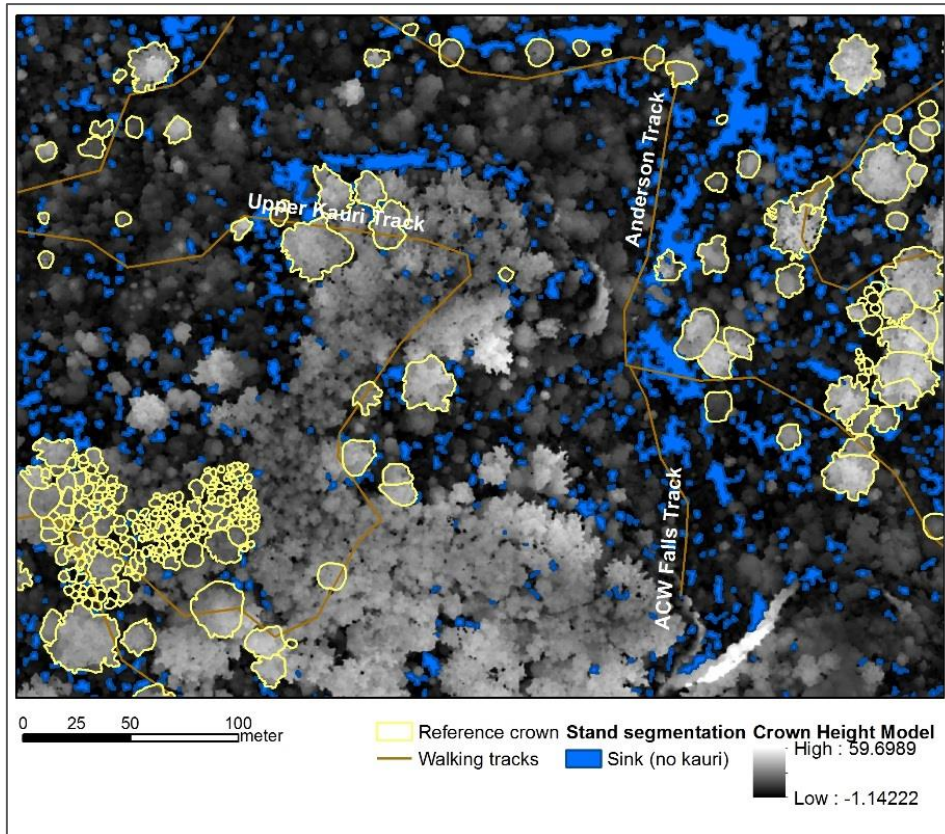
Stand segmentation in preparation for the crown segmentation:

- High stands and wide crown diameters including emerging high or wide crowns in the medium and low stands
- Medium stands with medium to small crown diameter including emerging medium crowns in the low stands
- Low stands with small and very small crown diameters

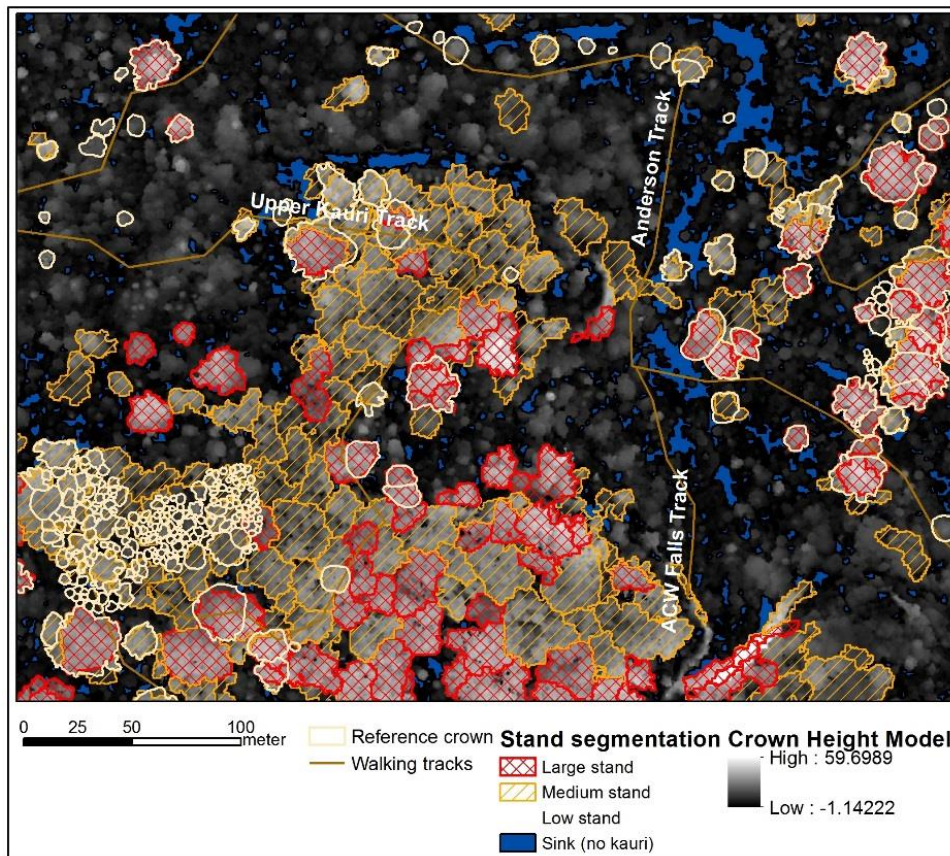
Stand segmentation to stratify reference crowns in size classes:

- High stands with a medium height > 21 m
- Low stands with a medium height <= 21 m

Tableau 13: Stand segmentation on LiDAR data



Map for step 1: Masking out sinks (blue). Reference crowns are marked in yellow.



Map for step3: Classification of the segments in three stand situations: Large (red), medium (orange) and small (transparent), sinks are marked in blue

3.4.2 Crown segmentation

The aim of the crown segmentation was to create a polygon for each crown that can be used in the crown-based kauri identification and the detection of stress symptoms.

Data preparation

In addition to the layers that were prepared for the stand segmentation, a contrast and variance raster on the CHM were used in the analysis. The reference crowns for the kauri classification were complemented with additional crown polygons that were edited in the circular plots and the monitoring plots from Auckland University on the LiDAR CHM.

Analysis

A test of an inverse watershed delineation [47] showed that it is difficult to identify a unique top point in larger kauri stands.

A combination of a multiresolution segmentation [48] and a region growing algorithm for the small stands was implemented in eCognition. The algorithm starts with a segmentation of the largest crowns and moves down level by level from a scale of 120 down to 5 for the smallest crowns. For each stand situation, additional sinks are identified, that function as breakpoints for the crown segmentation. A free-flowing unregulated segmentation and a regulated segmentation with defined shape and compactness values are combined on each level of the analysis. After the segmentation on each level, the correctly segmented polygons are selected in a supervised classification based on the reference crowns. The attributes for the classification are chosen with a J48 classifier in WEKA. The selected polygons are marked as finished results; the other polygons go back into the segmentation process for the next lower level.

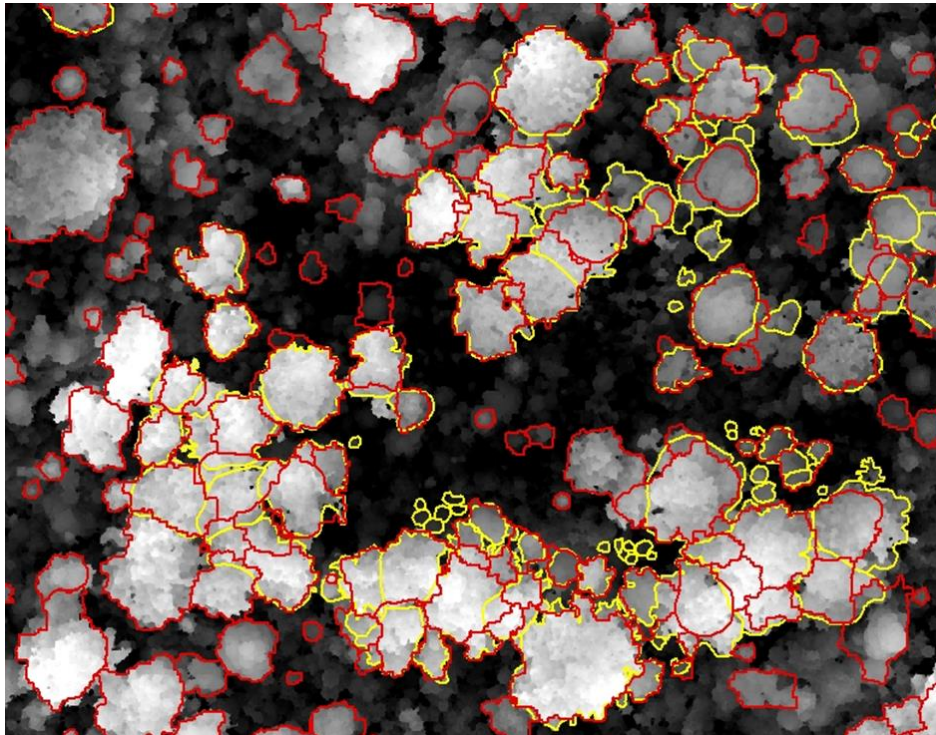
Progress

The stand segmentation was completed. The algorithms for the crown segmentation and a tile-based workflow, as well as a method for the accuracy assessment, were developed. So far, the best thresholds and attributes for the large to medium crowns were defined. The segmentation of small crown sizes is still under development.

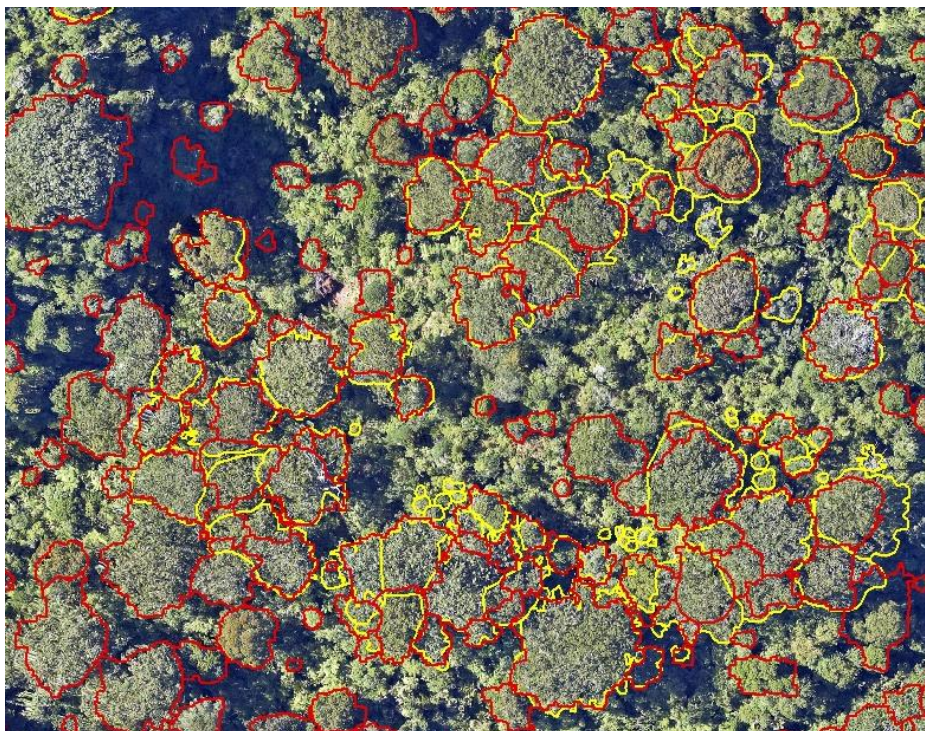
Findings

- A multiresolution segmentation in eCognition performed better for the crown segmentation than an inverse watershed segmentation. The multiresolution segmentation allows for the integration of texture layers and potentially also aerial and satellite images, given that these match the LiDAR data.
- While single standing trees and erased crowns are relatively easy to detect, the crown segmentation in denser stands with one height level is more challenging. Here the aim is to segment the crowns homogenous units that allow the detection of changes. The algorithm is adjusted to rather over-segment (several polygons per crown) than under-segment (one polygon covers several crowns).

Tableau 14: Crown segmentation on LiDAR data



Map: Automatically segmented crowns in eCognition on the LiDAR data. Scale 120 to 40. (background: LiDAR Crown Height Model from 2016).



Map: Same segmentation as above, with the aerial image from 2016 as background.

3.5 Main challenges and lessons learned

Delay in the data acquisition

All data sets that were ordered for this project were delayed, from 2 months for the first LiDAR data to over a year for both the hyperspectral, WV02 and 2nd LiDAR set. While the organizational problems might be reduced in future when everybody gains more experience, the cloudy and windy weather will be an issue and possibly even more so with the future effects of climate change. They require larger time windows for the acquisition.

Spatial accuracy of remote sensing data

The combination of different data acquisitions requires high spatial accuracy. The data should be orthorectified on a LiDAR-derived surface model (DSM) if they should be used in the automatic analysis. As an alternative to LiDAR data, the use of a DSM from stereo images should be tested.

Translation of stress symptoms to health categories

The stress symptom levels from 1 to 5 need to be interpreted to translate them into health categories. Apart from environmental aspects, the size of the crowns should be considered. The more open canopies of mature kauri crowns show a certain amount of branch material and internal shadows, even in a healthy state.

Reference data and analysis of symptom classes

In high and dense forest stands, high resolution RGB aerial images (≤ 15 cm pixels size) from the same season are better suited to assess stress symptoms in the canopy than the ground field data. An additional near-infrared band in addition to the RGB bands would make it easier to identify the state of symptom classes.

Spatial accuracy of field data and GPS data taken from a helicopter

The field survey data of Auckland Council could not be clearly located on the LiDAR crown height model, due to a low GPS accuracy (up to 15 m deviation).

To identify individual tree crowns on oblique photos taken from a helicopter also proved to be difficult and time-consuming, with deviation up to 90 m for the GPS points from the accurate position on the LiDAR crown height model (CHM).

Elaborate hyperspectral processing

The atmospheric correction and georeferencing of the hyperspectral was elaborate and required expert knowledge. In future acquisitions, the hyperspectral sensor should be flown under wind still conditions with high overlap between the stripes of at least 30%. Moreover, high accuracies of the on-board GPS and IMU are important. An updated sensor model and the latest laboratory measurements should be provided from the flight company.

4 Conclusions and outlook

Integrating remote sensing in a kauri monitoring strategy

The overall objectives of this study to automatically identify kauri trees and describe canopy stress symptoms with remote sensing data was achieved.

This study presents important findings on the use of remote sensing as part of a comprehensive kauri monitoring strategy. The identification of kauri trees or stands can be based on an airborne multispectral sensor with bands in the visible to far near-infrared range with high user's- and producer's accuracies over 94% in a pixel-based analysis. Alternatively, a crown-based approach to locate kauri crowns in a combination of LiDAR with multispectral data in the visible to NIR1 range can be used. It results in lower accuracies around 90%, depending on the spatial resolution and class definition. The automatic kauri detection with remote sensing data should be complemented with existing knowledge about kauri locations from fieldwork and airborne surveys.

For an object-based analysis, LiDAR data can be used for the segmentation of crowns. The minimum crown diameter for segmentation should be chosen according to the spatial resolution of the sensor used for stress detection. Stands with smaller crowns should be segmented in homogenous units.

While the best bands for kauri identification are located in the NIR2 spectral region, stress detection only requires standard bands in the visible to NIR1 spectral range up to 970 nm. A cost-efficient method for repeated monitoring of stress symptoms could be based on WorldView-2 satellite data for crown and canopy segments larger than 4 m in diameter with a correlation of 0.89 for five symptom levels. If possible, the attributes should include the maximum crown height based on LiDAR data for stratification in growth stages. Higher correlations for the stress detection (0.93) and smaller object sizes can be realized with more expensive airborne multispectral data, with bands in the green to NIR1 spectral range.

The acquisition planning should allow for regular monitoring as well as the flexibility to capture special events, such as the effects of storms or droughts. Matching high-resolution aerial images (< 15 cm) from the same season for representative stands can serve as a reference. After significant structural changes in the forest (e.g. caused by severe dieback or a storm), the LiDAR acquisition and segmentation of crowns and stands should be repeated. Dead and dying trees should be documented since they are soon overgrown.

Further details regarding the acquisition, the monitoring method and the presentation of the final maps should be developed in cooperation between the researchers, the management, including local Maori, and concerned stakeholder groups. This includes the choice of the multispectral sensor, which depends on the required spatial resolution, size of the area, terrain situation and available funding.

Support for other research areas and management decisions

Remote sensing allows to detect early changes in the leaf composition or top branches that are difficult to map in the field. It helps to set priorities for the field sampling and measures, locate trees that are non-symptomatic in infected stands to test for resistance, and monitor the effectiveness of measures like the closing of paths. It can help to narrow down the cause of stress symptoms and correlations to a possible PA infection by analyzing the change of stress symptom patterns over time and spectral indices related to different types of stress. Remote sensing can also help to better understand the extent, the speed, pathways of the infection, especially when changes in stress symptoms can be documented over a longer period, e.g. with historical satellite images.

Suggestions for further research

Further research should prioritize the use of LiDAR data for an automatic crown- and stand-segmentation and for its contribution to identifying kauri crowns in combination with multispectral data. As part of this study, a method for an automatic crown-segmentation based on LiDAR height models was developed, and the identification of kauri with LiDAR and WV2 data was tested. These analyses showed promising results and should be further developed.

The use of time series over different seasons for kauri identification, especially the bright green spring aspect, should be analyzed. Change detection in time series for the same season can help to distinguish the progress of infection from other stress factors like drought and to identify possible transmission pathways. Higher spatial resolution data (e.g. from UAV), quantitative measurements of stress reactions in crowns and controlled experiments in pot trials could help to obtain a better understanding of canopy stress responses and serve as a reference for satellite analysis.

A better understanding of the spectral characteristics and stress responses in other species is necessary for the analysis of mixed stands and wall-to-wall forest health monitoring. Crown spectra from an airborne hyperspectral image can be used for spectral unmixing to analyze the species composition in heterogeneous stands. This approach can also improve the use of optical remote sensing data with a lower spatial resolution, such as the freely available Sentinel-2 and Landsat-8 sensor systems.

In combination with the higher frequency and longer duration of drought periods caused by climate change, kauri dieback disease could contribute to a shift in species composition in New Zealand kauri forests. Long-term monitoring should include all the main canopy species and focus on the composition and functions of the forest ecosystem.

5 Abbreviations

CHM	Crown Height Model (a ground normalized DSM)
DBH	Stem diameter at breast height
DSM	Digital Surface Model
DTM	Digital Terrain Model
FWHM	Full width at half maximum
GCP	Ground Control Point
GNSS	Global Navigation Satellite System
GPS	Global Positioning System
LiDAR	Light Detection and Ranging
MNF	Minimum Noise Fraction Transformation
MPI	Ministry for Primary Industries
NIR	Near-infrared
PAN	Panchromatic, black and white band
PC	Principal component
PA	Phytophthora agathidicida
RPC	Rational Polynomial Coefficient
SWIR	Short Wave Infrared
VIS	Visible

6 References

1. Meiforth, J.J.; Buddenbaum, H.; Hill, J.; Shepherd, J.; Norton, D.A. Detection of New Zealand Kauri Trees with AISA Aerial Hyperspectral Data for Use in Multispectral Monitoring. *Remote Sensing* **2019**, *11*, 2865.
2. Meiforth, J.J., Buddenbaum H. , Hill J., Shepherd J. Monitoring of Canopy Stress Symptoms in New Zealand Kauri Trees Analyzed with AISA Hyperspectral Data. . *Remote Sensing* **2020a**.
3. Meiforth, J.J.; Buddenbaum, H.; Hill, J.; Shepherd, J.D.; Dymond, J.R.J.R.S. Stress Detection in New Zealand Kauri Canopies with WorldView-2 Satellite and LiDAR Data. **2020b**, *12*, 1906.
4. Steward, G.A.; Beveridge, A.E. A review of New Zealand kauri (*Agathis australis* (D. Don) Lindl.): its ecology, history, growth and potential for management for timber. *New Zealand Journal of Forestry Science* **2010**, *40*, 33-59.
5. Beever, R.E.; Waipara, N.W.; Ramsfield, T.D.; Dick, M.A.; Horner, I.J. Kauri (*Agathis australis*) under threat from *Phytophthora*. *Phytophthoras in Forests and Natural Ecosystems* **2009**, *74*.
6. Gadgil, P.D. *Phytophthora heveae*, a pathogen of Kauri. *New Zealand journal of forestry science* **1974**, *4*, 59-63.
7. Bellgard, S.; Weir, B.; Pennycook, S.R.; Paderes, E.P.; Winks, C.; Beever, R.E.; Williams, S. Specialist phytophthora research: Biology, pathology, ecology and detection of PTA. Final report for the New Zealand Ministry for Primary Industries: 2013.
8. Bellgard, S.E.; Weir, B.S.; Pennycook, S.R.; Paderes, E.P.; Winks, C.; Beever, R.E. Specialist Phytophthora Research: Biology. Pathology Ecology and Detection of PTA. *MPI Contract* **2013**, *11927*.
9. Scott, P.; Williams, N. Phytophthora diseases in New Zealand forests. *NZ Journal of Forestry* **2014**, *59*, 15.
10. Beauchamp, A. The detection of Phytophthora Taxon “*Agathis*” in the second round of surveillance sampling—With discussion of the implications for kauri dieback management of all surveillance activity. *Report prepared for Ministry for Agriculture & Forestry on behalf of Kauri Dieback Joint Agency* **2013**, 38.
11. MPI. *Kia toitu he kauri – keep kauri standing. New Zealand's strategy for managing kauri dieback disease.*; <https://www.kauridieback.co.nz/media/1393/kauri-diebackstrategy-2014-final-web.pdf>, 2014; p 24.
12. Waipara, N.; Hill, S.; Hill, L.; Hough, E.; Horner, I. Surveillance methods to determine tree health, distribution of kauri dieback disease and associated pathogens. *New Zealand Plant Protection* **2013**, *66*, 235-241.
13. Jamieson, A.; Bassett, I.; Hill, L.; Hill, S.; Davis, A.; Waipara, N.; Hough, E.; Horner, I. Aerial surveillance to detect kauri dieback in New Zealand. *New Zealand Plant Protection* **2014**, *67*, 60-65.
14. Singers, N.; Osborne, B.; Lovegrove, T.; Jamieson, A.; Boow, J.; Sawyer, J.; Webb, C. Indigenous terrestrial and wetland ecosystems of Auckland. Auckland Council Retrieved from <http://www.knowledgeauckland.org.nz>, accessed on 20/07/2019: Auckland, New Zealand, 2017.
15. Jamieson, A. Aerial surveillance to detect kauri dieback in New Zealand. *New Zealand Plant Protection* **2014**, *67*, 60-65.
16. Chappell, P.R. The climate and weather of Auckland. *NIWA SCIENCE AND TECHNOLOGY SERIES, Auckland* **2012**, *60*.
17. LINZ. LINZ Data Service - Mapserver for geospatial data hosted by Land Information New Zealand. . Available online: (accessed on
18. NIWA. The National Climate Database. Available online: (accessed on
19. AC. Forest baseline data (Nov 2009 – Dec 2014). Vegetation data relating to the first 6 years of baseline measures of forest monitoring plots on public land. Council, A., Ed. 2015.
20. AC. Walking tracks in the Waitakere Ranges Council, A., Ed. 2015.
21. MPI. Map data (shp files) for PTA positive sampling sites (updated 23/01/2019) and the natural range of kauri distribution. Provided on the 13/02/2020. Regulations for use and liability are stated on the map. https://www.kauridieback.co.nz/media/2037/kauri-dieback-distribution_20190930_350dpi.jpg Ministry for Primary Industries, Biosecurity, Wellington. **2020**.

22. ESRI. World Topographic Map - WMTS service. Sources: Esri, HERE, Garmin, Intermap, INCREMENT P, GEBCO, USGS, FAO, NPS, NRCAN, GeoBase, IGN, Kadaster NL, Ordnance Survey, Esri Japan, METI, Esri China (Hong Kong), © OpenStreetMap contributors, GIS User Community. **2020**.
23. LINZ. NZ Topo50. Topographical Map for New Zealand. . Imported on April 14, 2019 from 445 GeoTIFF sources in NZGD2000 / New Zealand Transverse Mercator 2000. ed.; <https://www.linz.govt.nz/land/maps/topographic-maps/topo50-maps>. Accessed on 20/07/2019: 2019.
24. Auckland Council. Helicopter Survey on Kauri Dieback in the Waitakere Ranges. Conducted by Alastair Jamieson, Wild Earth Media in January and February 2016. **2016**.
25. Burns, B. Survey data of permanent vegetation plots in the Waitakere Ranges. Auckland University. **2016**.
26. NZPCN. Photos from the website of the New Zealand Plant Conversation Network. The photographers are: Department of Conversation, Jeremy Rolfe, Wayne Bennett and John Smith-Dodsworth. Download 2015. **2015**.
27. Jeffreys, H. An invariant form for the prior probability in estimation problems. *Proceedings of the Royal Society of London. Series A. Mathematical and Physical Sciences* **1946**, *186*, 453-461.
28. van der Linden, S.; Rabe, A.; Held, M.; Jakimow, B.; Leitão, P.J.; Okujeni, A.; Schwieder, M.; Suess, S.; Hostert, P. The EnMAP-Box—A toolbox and application programming interface for EnMAP data processing. *Remote Sensing* **2015**, *7*, 11249-11266.
29. Khosravipour, A.; Skidmore, A.K.; Isenburg, M. Generating spike-free digital surface models using LiDAR raw point clouds: A new approach for forestry applications. *International journal of applied earth observation and geoinformation* **2016**, *52*, 104-114.
30. Weir, B.S.; Paderes, E.P.; Anand, N.; Uchida, J.Y.; Pennycook, S.R.; Bellgard, S.E.; Beever, R.E. A taxonomic revision of Phytophthora Clade 5 including two new species, *Phytophthora agathidicida* and *P. cocois*. *Phytotaxa* **2015**, *205*, 21-38.
31. Hurst, J.; Allen, R. A permanent plot method for monitoring indigenous forests-expanded manual, version 4. *Landcare Research Contract report LC0708/028* **2007**.
32. DOC. *The Foliar Browse Index field manual. An update of a method for monitoring possum (Trichosurus vulpecula) damage to forest communities*; Christchurch, New Zealand, 2014; p 56.
33. Zarco-Tejada, P.J.; Berjón, A.; López-Lozano, R.; Miller, J.R.; Martín, P.; Cachorro, V.; González, M.; De Frutos, A. Assessing vineyard condition with hyperspectral indices: Leaf and canopy reflectance simulation in a row-structured discontinuous canopy. *Remote Sensing of Environment* **2005**, *99*, 271-287.
34. Aparicio, N.; Villegas, D.; Araus, J.; Casadesus, J.; Royo, C. Relationship between growth traits and spectral vegetation indices in durum wheat. *Crop Sci.* **2002**, *42*, 1547-1555.
35. Gitelson, A.A.; Merzlyak, M.N. Remote estimation of chlorophyll content in higher plant leaves. *International Journal of Remote Sensing* **1997**, *18*, 2691-2697.
36. Birth, G.S.; McVey, G.R. Measuring the Color of Growing Turf with a Reflectance Spectrophotometer 1. *Agron. J.* **1968**, *60*, 640-643.
37. Peñuelas, J.; Filella, I.; Biel, C.; Serrano, L.; Save, R. The reflectance at the 950–970 nm region as an indicator of plant water status. *International journal of remote sensing* **1993**, *14*, 1887-1905.
38. MPI. Airbone LiDAR and RGB aerial images in the Waitakere Ranges. Flown by AAM-New Zealand for the Ministry of Primary Industries. **2016**.
39. Datt, B. Remote sensing of chlorophyll a, chlorophyll b, chlorophyll a+ b, and total carotenoid content in eucalyptus leaves. *Remote Sensing of Environment* **1998**, *66*, 111-121.
40. Rouse Jr, J.W.; Haas, R.H.; Schell, J.; Deering, D. Monitoring the vernal advancement and retrogradation (green wave effect) of natural vegetation. *NASA Gsfct Type Report; Texas A&M University: College Station, TX, USA* **1973**.
41. Gamon, J.; Surfus, J. Assessing leaf pigment content and activity with a reflectometer. *The New Phytologist* **1999**, *143*, 105-117.
42. Green, A.A.; Berman, M.; Switzer, P.; Craig, M.D. A transformation for ordering multispectral data in terms of image quality with implications for noise removal. *IEEE Transactions on geoscience and remote sensing* **1988**, *26*, 65-74.

43. Metternicht, G. Vegetation indices derived from high-resolution airborne videography for precision crop management. *International Journal of Remote Sensing* **2003**, *24*, 2855-2877.
44. Haralick, R.M.; Shanmugam, K.; Dinstein, I.H. Textural Features for Image Classification. *Systems, Man and Cybernetics, IEEE Transactions on* **1973**, *SMC-3*, 610-621, doi:10.1109/TSMC.1973.4309314.
45. Adeline, K.; Chen, M.; Briottet, X.; Pang, S.; Paparoditis, N. Shadow detection in very high spatial resolution aerial images: A comparative study. *ISPRS Journal of Photogrammetry and Remote Sensing* **2013**, *80*, 21-38.
46. Khosravipoura, A.; Skidmore, A.K.; Isenburg, M. Generating spike-free digital surface models using LiDAR raw point clouds: A new approach for forestry applications. *International Journal of Applied Earth Observation and Geoinformation* **2016**, *52*, 104 – 114.
47. Zhao, K.; Popescu, S. Hierarchical watershed segmentation of canopy height model for multi-scale forest inventory. *Proceedings of the ISPRS working group "Laser Scanning* **2007**, 436-442.
48. Baatz, M.; Schäpe, A.; Schmidt, G.; Athelougou, M.; Binnig, G. Cognition network technology: object orientation and fractal topology in biomedical image analysis. Method and applications. In *Fractals in Biology and Medicine*, Springer: 2005; pp. 67-73.
49. Council, A. 0.075m Urban Aerial Photos (2017), RGB, Waitakere Ranges. <https://data.linz.govt.nz/layer/95497-auckland-0075m-urban-aerial-photos-2017/> (accessed on 12/04/2019). **2017**.

7 Appendix

7.1 Support for the project

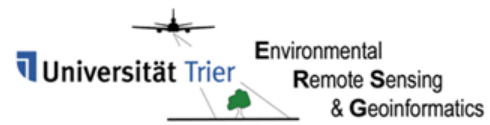
The Kauri Dieback Program under the Ministry for Primary Industries financed the main research costs, including most of the remote sensing data. <https://www.kauridieback.co.nz/>



The University of Canterbury (UC) provided the main scholarship (UC doctoral) to cover the living costs for three years, some of the field equipment and a laptop. The main supervisor in New Zealand, Professor David Norton, is based at the School of Forestry at UC.



The University of Trier provided most of the software licenses. The main supervisor in Germany, Professor Joachim Hill and the co-supervisor Dr. Henning Buddenbaum are based at Department of environmental Remote Sensing and Geoinformatics



Auckland Council provided the main support during the fieldwork in the Waitakere Ranges, including data, a field assistant, safety backups and accommodation. <https://www.aucklandcouncil.govt.nz/>



FrontierSI (former CRCSI) financed two stripes of LiDAR data flown with the sensor that was used in Northland. They also helped with a top-up scholarship for private living costs. <https://frontiersi.com.au/>



Free satellite data was provided through image grants from **Digital Globe** and **Planet Labs** (former Blackbridge). <https://www.digitalglobe.com/>



Manaaki Whenua Landcare Research provided expensive field equipment, a field spectrometer, a mapping grade GPS and a sun-photometer. Dr James Shepherd was a co-supervisor on the project. <https://www.landcareresearch.co.nz/>



Rapidlasso and **Harris Geospatial** provided 3 months trial licenses for LAsTools respective ENVI FLAASH. <https://rapidlasso.com/> <https://www.harrisgeospatial.com/>



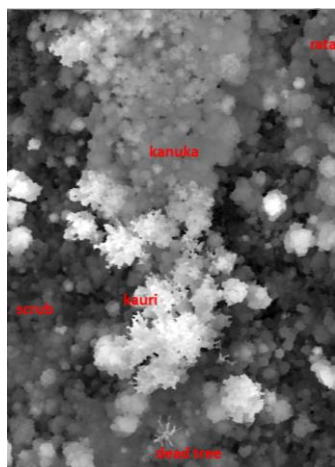
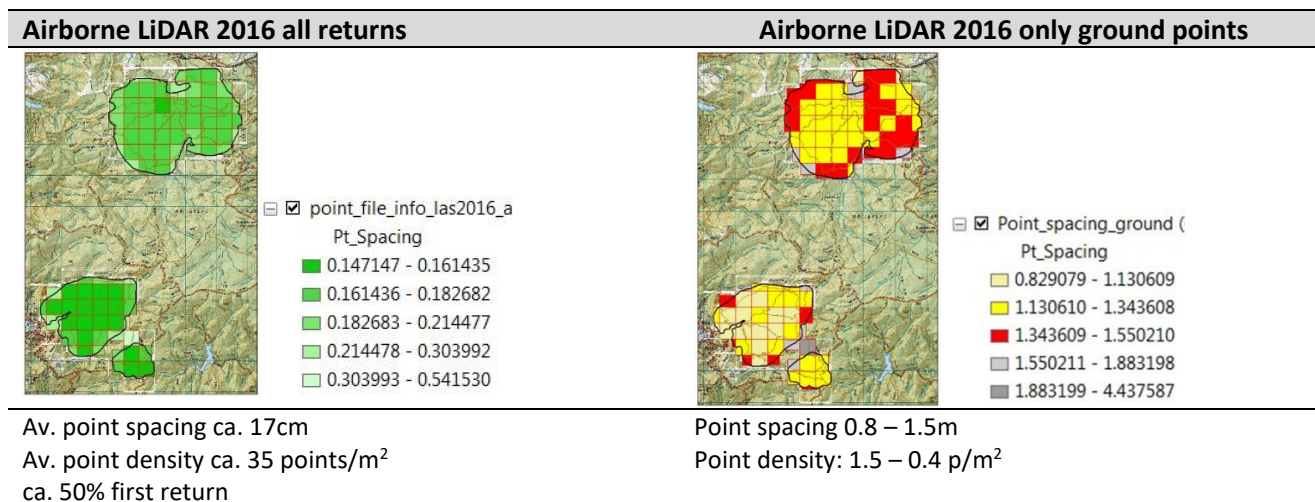
Fredrik Hjelm, the founder of **the living tree company** and **Joanne Peace**, were excellent assistants during the field work. They showed extraordinary commitment, reliability, botanical knowledge and technical understanding. <http://thelivingtreecompany.co.nz/>



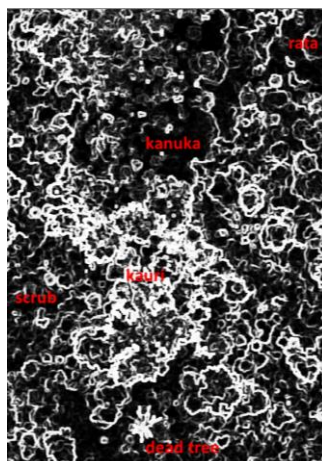
7.2 LiDAR data

Flight attributes	Jan-2016*	Jan-2018
Area	All 3 study sites	2 stripes over the Cascades
Date	30th of January 2016	14 th of January 2018
Sensor (HZ)	Q1560 LiDAR sensor (400 kHz, 58° FOV)	360 Hz
Swath Width	Ca. 400m	1154m
Overlap	55% side overlap	30%
Single flight line pulse density	5 pulses / sqm	3.35 pts/m ²
Average point density	15 pulses /sqm > 35 returns / sqm	5.13 returns / sqm
Average point spacing	0.17 m	0.44 m
Ground avg. pnt density	0.5 – 1.6 returns / sqm	0.44 returns / sqm
Ground avg. pnt spacing	0.4 -1.5 m	1.5 m
Horizontal accuracy	±0.50m Standard Error (68% conf. level)	No information provided
Vertical accuracy	±0.10m Standard Error (68% conf. level)	No information provided
Waveform	Yes	No
Pulse footprint	NaN	0.23 m
Classification	ICSM Level 1: Default, Ground, Low vegetation (0-0.3m), Medium Veg. (0.3-2m), High Veg. (>2m), Buildings, Low/high points.	Ground <> Non-Ground

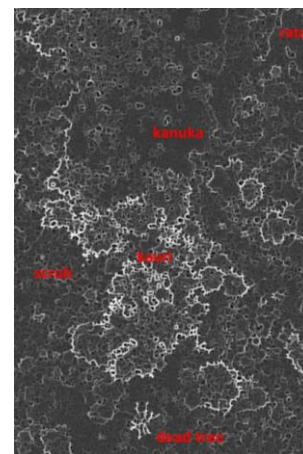
*MPI 2016: Airborne LiDAR data for Kauri Dieback Project in the Waitakere Ranges. Flown 30.01.2016



Crown Height Model



Variance


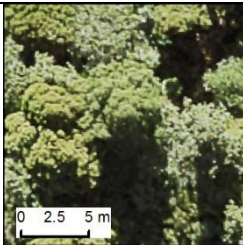
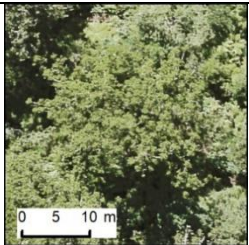

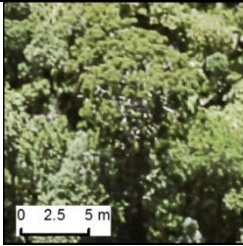


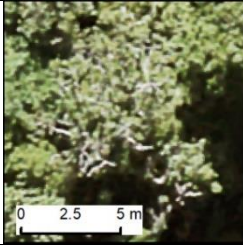


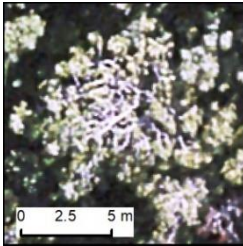
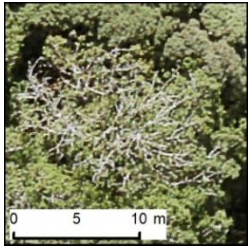
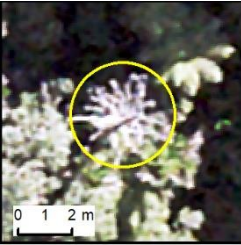
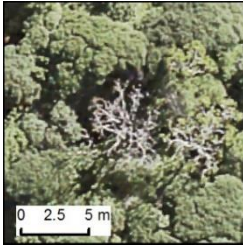
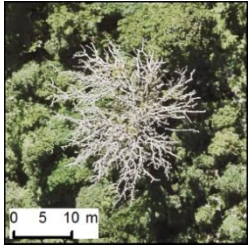


Maximum Curvature

Figure: Illustration of LiDAR attributes for different canopy vegetation

7.3 Assessment scheme for stress symptoms in kauri crowns

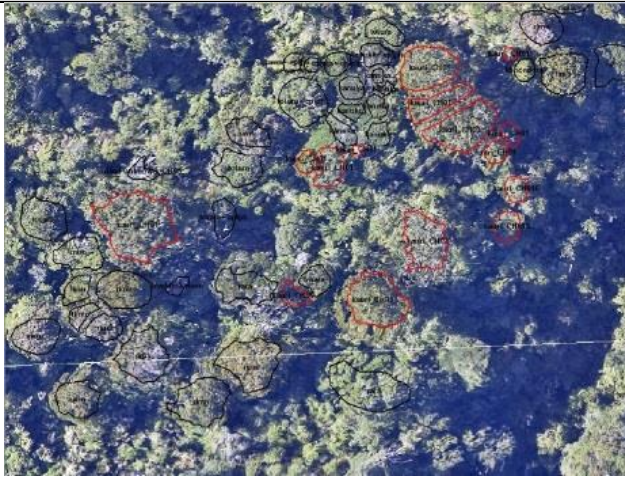
Table Assessment scheme for stress symptoms in kauri crowns based on RGB aerial images [38,49] for five canopy stress symptom classes and three crown sizes.

Symptom class	Description	Size small ¹	Size medium ¹	Size large ¹
Value 1 No Symptoms	Leaves: green, green/blue; Canopy density: dense, no to small gaps; Bare branches: <1%			
Value 2 First Symptoms / Open Crowns	Leaf colour: green to yellowish; Canopy density: small gaps; Bare branches: 1 to 5% (small branches)			
Value 3 Medium Symptoms	Leaves: green with yellow or brown; Canopy density: small to medium gaps visible; Bare branches: 5%–30%			
Value 4 Severe Symptoms	Leaves: yellow-green to brown; Canopy density: sparse, many gaps, understory partly visible; Bare branches: >=30% visible as linear structures Epiphytes and climbers possible			
Value 5 Dead Trees	Leaves: dead, brown leaves possible Epiphytes and climbers possible; Canopy density: Gaps and understory visible, Bare branches: 100%, dead branches visible as linear structures			

¹ The crown size classes are defined according to their mean crown diameter, see 1. Non-symptomatic large and medium crowns with open canopies were given the value 1.5 in the analysis.

7.4 Kauri detection – images and maps

**Open stand with high trees
(Kauri Grove Track)**

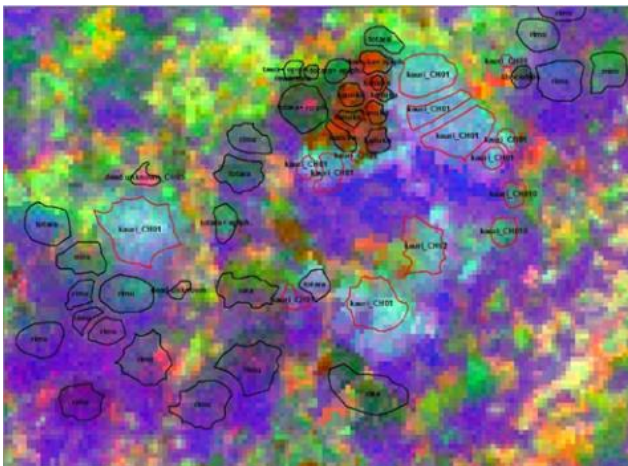


Aerial image

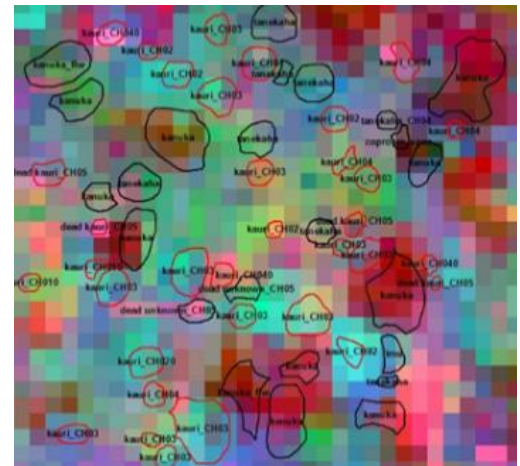
**Dense small stand with infected trees
(Maungaroa Ridge Track)**



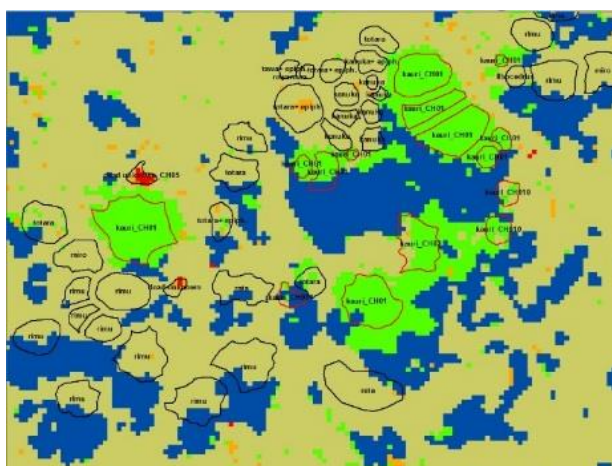
Aerial image



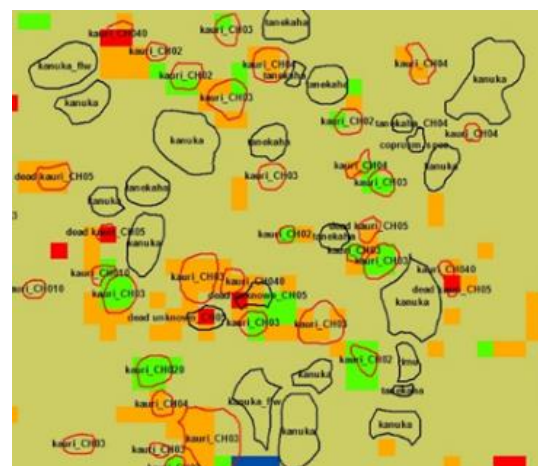
MNF compression hyperspectral



MNF compression hyperspectral



Classified image on 5 multispectral bands for 5 classes. The image was post processed with a majority filter with different filter settings according to the stand situation.



Classified image on 5 multispectral bands for 5 classes. The image was post processed with a majority filter with different filter settings according to the stand situation.

- Kauri mask
 - unclassified (shadow)
 - Kauri CH123 (healthy to slight symptoms)
 - Kauri CH34 (symptoms)
 - Kauri/other CH45 (severe symptoms or dead)
 - other